DFUB 20/94

MAGNETIC MONOPOLES SEARCHES

GIORGIO GIACOMELLI
Dipartimento di Fisica dell'Università di Bologna
I.N.F.N., Sezione di Bologna

Invited lectures at the 1994 Lake Louise Winter Institute

ABSTRACT

The main aim of these lectures is to give a broad overview of the basic properties of magnetic monopoles and of their experimental searches.

1. Introduction

The concept of magnetic monopole may be traced back to the origin of magnetism. The first scientific account of magnetic materials is a letter, written by the French military engineer Petrus Peregrinus (Pierre) De Maricourt, describing the lines of force around a lodestone and noting that they started and terminated at two points, which he called the north and south poles *. All subsequent observations confirmed that all magnetic objects are dipoles.

At the beginning of the 19th century there were discussions (and experiments) concerning the magnetic content of matter and some speculations about the possible existence of isolated magnetic charges.

In 1931 Dirac introduced the magnetic monopole in order to explain the quantization of the electric charge, which follows from the existence of at least one free magnetic charge. Dirac established the basic relation between the elementary electric charge e and the magnetic charge g. The existence of magnetic charges and of magnetic currents would symmetrize in form Maxwell's equations, but the smallest magnetic charge is predicted to be much larger than the smallest electric charge [1]. These reasonings introduced what we may now call the "classical Dirac magnetic monopole". There was no prediction for the monopole mass; a guess, assuming that the classical electron radius be equal to the "classical monopole radius" yields $m_M \simeq g_D^2 m_e/e^2 \simeq 4700 m_e \simeq 2.4$ GeV.

From 1931 many searches were made for "classical Dirac monopoles" at every new accelerator, which opened up a new energy region. Monopoles were thought to be produced in high-energy reactions of the type

$$e^+ + e^- \to g + \bar{g}, \qquad p + p \to p + p + g + \bar{g}, \qquad \bar{p} + p \to g + \bar{g}, \tag{1}$$

where g is a monopole and $\bar{g}$ is an antimonopole. The searches were made with relatively simple set-ups; searches of this type are still going on at the newest accelerators.

* Peter Peregrinus, Epistula de Magnete. Epistle of P.P. of Maricourt to S. Foncaucourt written in 1269; translated from latin to english by S.P. Thompson in 1902

Around 1974 it was realized that the electric charge is naturally quantized in unified gauge theories of the basic interactions in which electromagnetism is embedded in a spontaneously broken gauge theory and that such unified theories imply the existence of magnetic monopoles, with calculable properties. In the context of the Grand Unification of strong and electroweak interactions (GUT), the magnetic monopoles appear at the transition corresponding to the spontaneous breaking of the unified group into subgroups, one of which is U(1) [2,3]. The monopole mass is related to the mass of the X, Y particles, which are the carriers of the unified interaction, $m_M \geq m_X/G$, where G is the dimensionless unified coupling constant. In GUT one has $m_X \simeq 10^{14} - 10^{15}$ GeV and $G \simeq 0.025$; consequently $m_M > 10^{16} GeV \simeq 0.02 \mu g$. This is an enormous mass; therefore, magnetic monopoles cannot be produced at any man made accelerator, existing or conceivable. They could only be produced in the first instants of the Universe. Some GUT's offer the possibility of lighter magnetic monopoles. If also gravity is brought into the unifying picture, for instance in the form of Kaluza-Klein theories, then monopoles could be much more massive [4,5], $m_M \geq 10^{19}$ GeV. Large masses are also obtained in SuperSymmetric theories.

The application of the simplest GUT theories to the standard early universe scenario yields too many monopoles, while inflationary scenarios lead to a very small number. Thus gauge theories of the unified interactions demand the existence of magnetic monopoles, but the prediction of the monopole mass is uncertain by several orders of magnitude, the magnetic charge could be between one and several Dirac units and the expected flux could vary from an extremely small value to a sizable and observable flux. Experimenters should thus have an open mind.

Magnetic monopoles of lowest mass are expected to be stable, since magnetic charge should be conserved like electric charge. Therefore, the monopoles produced in the early Universe should still be around as cosmic relics, whose kinetic energy has been strongly affected by their travel through galactic magnetic fields.

After the 1982 excitement due to a monopole candidate [6], there was rapid progress in analysing various types of astrophysical and cosmological bounds and in detailed studies of the energy losses of monopoles in matter. The most direct method of searching for GUT monopoles is to search them in the penetrating cosmic radiation. GUT poles should be characterized by low velocities and relatively large energy losses. Experimental flux upper limits were obtained with a large variety of detectors, which quickly increased in size and complexity. Now only few large underground detectors are in use.

The aim of these lectures is to give a broad overview of experimental monopole searches. Section 2 reviews the basic properties of magnetic monopoles. The interaction of monopoles in matter is given in Section 3, while the various methods of monopole detection are described in Section 4. Searches for classical and GUT monopoles are described in Sections 5 and 6, respectively. The monopole catalysis of proton decay is briefly discussed in Section 7. Other types of searches are described in Section 8. Outlook and conclusions are given in Section 9. For more details, the reader may consult specialized review papers [4,5] and conference summaries [7,8].

The Gauss CGS symmetric system of units will be used throughout.

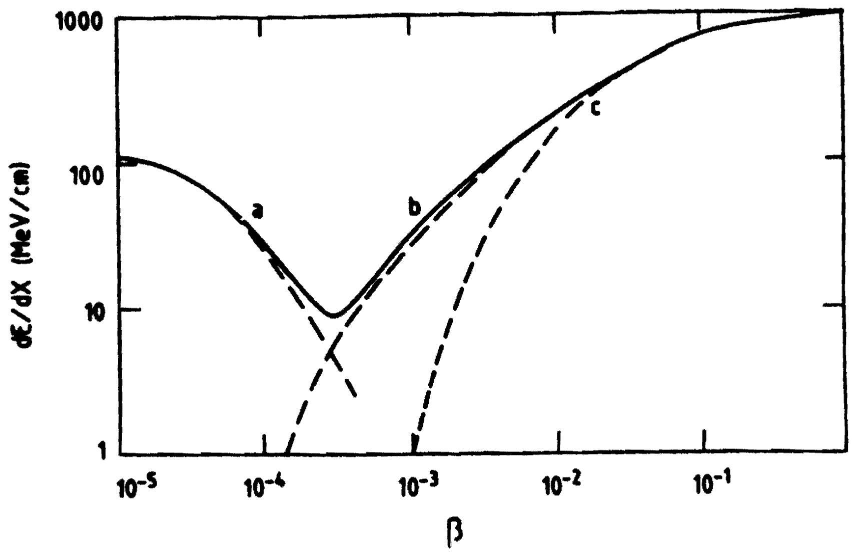

Figure 1 - The energy losses, in MeV/cm, of magnetic monopoles in liquid hydrogen as a function of β [9-14]. Curve a) corresponds to elastic monopole-hydrogen atom scattering; curve b) corresponds to interactions with level crossings [10]; curve c) describes the ionization energy loss.

2. Summary ot the properties of magnetic monopoles

2.1. Properties based on the Dirac relation

In this Section the consequences of the Dirac relation

$$eg = n\hbar c/2 \tag{2}$$

will be summarized.

- *Magnetic charge.*

If $n = 1$ and the basic electric charge is that of the electron one has:

$$g_D = \frac{\hbar c}{2e} = \frac{137}{2}e = 3.29 \cdot 10^{-8} \quad CGS \quad units \tag{3}$$

If the elementary electric charge is that of quarks with charge $1/3$, one would have an elementary magnetic charge 3 times larger. A similar situation arises if $|n| > 1$.

- *Coupling constant.*

In analogy with the fine-structure constant, $\alpha = e^2/\hbar c \simeq 1/137$, one may define a dimensionless magnetic-coupling constant

$$\alpha_g = \frac{g_D^2}{\hbar c} = \frac{e^2}{\hbar c} \cdot \frac{g_D^2}{e^2} \simeq \frac{1}{137} \cdot \left(\frac{137}{2}\right)^2 = 34.25 \tag{4}$$

Notice that α_g is larger than 1; this leads to several complications.

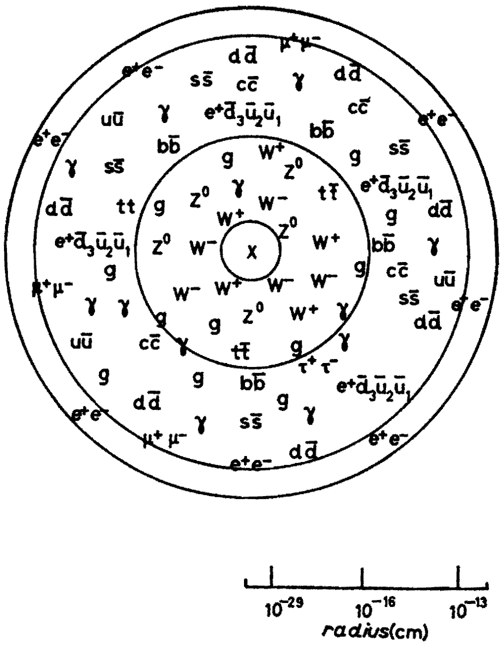

Figure 2 - Illustration of the GUT monopole structure. The sketch illustrates various regions corresponding to: i) Grand Unification ($r \sim 10^{-29}$ cm; inside this core one may find virtual X- and Y- particles); ii) electroweak unification ($r \sim 10^{-16}$ cm; inside one may find virtual $W^{\pm}$, Z); iii) the confinement region ($r \sim 10^{-13} cm$; inside one may find virtual γ, gluons and a condensate of fermion-antifermion, 4 fermion virtual pairs); iv) for radii larger than few fm one has the field of a point magnetic charge, $B = g/r^2$ [5].

- *Energy W acquired in a magnetic field B by a pole with* $g = g_D$:

$$W = g_D B \ell = 20.5 \quad keV/G\ cm. \tag{5}$$

(the loss is given for $B = 1$ G and $\ell = 1$ cm). Because of the large g-value, monopoles acquire large energies even in modest magnetic fields acting over short distances. In a coherent galactic-length ℓ, with $\ell \simeq 1$ kpc and $B \simeq 3\mu G$, the energy gained by a monopole is:

$$W_G = WB\ell = 20.5 \frac{keV}{G\ cm}(3{\times}10^{-6} G)(3{\times}10^{21}\ cm) = 1.8{\times}10^{17}\ keV = 1.8{\times}10^{11}\ GeV$$

- *Energy losses in matter*

The energy losses of fast, slow and very slow monopoles in matter are discussed in Section 3. A fast monopole with magnetic charge g_D and velocity $v = \beta c$ behaves like an equivalent electric charge $(Ze)_{eq} = g\beta$. Fig. 1 shows the behaviour of the energy losses of monopoles in liquid hydrogen.

- *Trapping of monopoles in ferromagnetic materials.*

Magnetic monopoles may be trapped in bulk paramagnetic and ferromagnetic materials by an image force, which, in ferromagnetic materials, may reach the value of $\simeq 10$ eV/Å; the binding energy in paramagnetic materials is $\simeq 200$ eV [11,14].

2.2. *Properties of GUT monopoles*

- *Mass.*

As stated, Grand Unified Theories (GUT) of electroweak and strong interactions predict the existence of magnetic monopoles with large masses. Electrically charged monopoles (dyons) may arise as quantum-mechanical excitations of GUT poles or as $M-p$, M-nucleus composites. In the following we shall assume a mass $m_M \simeq 10^{17}$ GeV for the stable monopole; but there could be poles with higher and lower masses.

The GUT magnetic pole is pictured as having (see Fig. 2):

- a core with a radius $r_c \simeq 1/m_X \simeq 10^{-29} cm$ ($10^{-32} cm$ for $m_M \simeq 10^{19} GeV$);
- a region up to $r \simeq 10^{-16} cm$, where virtual W^+, W^- and Z^o may be present;
- a confinement region with $r^{conf} \simeq 1 fm$;
- a fermion-antifermion condensate region up to $r_f \simeq 1/m_f$; the condensate may contain 4-fermion baryon-number-violating terms up to the confinement radius;
- for r larger than $\simeq 3fm$ the GUT pole behaves as a point Dirac monopole, which generates a magnetic field $B = g/r^2$.

One may think that going through the GUT monopole one sees a "small universe", with different regions full of different virtual particles.

3. Interaction of monopoles with matter

3.1. *Introduction*

It is obviously important to know if the quantity and quality of energy lost by magnetic monopoles in particle detectors is adequate for monopole detection. Classical poles should have relatively small masses, so that acceleration to relativistic velocities is inevitable. For such velocities the energy losses are $(g_D/e)^2 \simeq 4700$ times the energy loss of a minimun ionizing electric charge. Thus the energy loss of a classical pole would be enormous, and the pole may be easily detected by almost any kind of particle detector. Instead GUT poles have large masses and are expected to have relatively low velocities, $10^{-4} < \beta < 10^{-1}$. The study of the energy losses of slow moving monopoles becomes thus of great interest.

There is also interest in determining the rate at which monopoles lose energy in various astrophysical objects, such as the Earth and the stars, in order to establish the likelihood of primordial poles of being trapped in these objects. Classical monopoles would lose quickly their energy and could easily stop at the surface of the Earth. Instead GUT poles would only stop in the largest celestial bodies [9].

The interaction of the monopole magnetic charge with nuclear magnetic dipoles could lead to the formation of M-nuclei bound systems, with binding energies in the range ($1 \div 100$) keV and with typical sizes of the order of 10 fm. Since the scales of these systems are approximately the same as those of mesic atoms, the name "monopolic atoms" has been used in the literature. Furthermore, monopoles and atomic nuclei may be bound together by electrons, in a way similar to the chemical binding of molecules. These systems, referred to as "monopolic molecules", may have typical linear sizes of the order of 1 Å and binding energies of the order of 1 eV. The formation of monopolic atoms and molecules may affect the energy loss in matter and the cross-section for the monopole catalysis of proton decay.

The long-range interaction of a magnetic pole with a fermion is due to the "magneto-static" interaction between the pole magnetic charge and the dipole-magnetic moment of the fermion. The interaction energy is

$$W_D = -\vec{\mu}_e \cdot \vec{B} = \hbar^2/4m_e r_e^2. \tag{6}$$

For an electron at $r_e = a_o$ one has $W_D \simeq 7$ eV, which is comparable to the binding energy of an atom; thus one expects a sizable deformation of an atomic system when a monopole passes inside or close to an atom. For a proton ($\mu_p = 2.8e\hbar/2m_p c$) at a distance $r = 1\ fm$ from the monopole one has $W_D = 2.8\hbar^2/4m_p r^2 \simeq 29 MeV$, a value larger than the binding energy of nucleons in nuclei; thus one expects deformations of the nucleus when a monopole passes close to it.

For a nucleus with spin s_A and magnetic moment $\vec{\mu}_A$ the dipole Hamiltonian $W_D = -\vec{\mu}_A \cdot \vec{B}$ is attractive for a suitable spin orientation. One can have monopole-nucleus bound states if the total Hamiltonian, inclusive of the centrifugal barrier part, is attractive. This is the case for nuclei with large and positive anomalous magnetic moments, like proton, aluminium, etc.

Monopole-proton bound states may be produced via radiative capture

$$M + p \rightarrow (M + p)_{bound} + \gamma \tag{7}$$

with cross-sections of the order of $(1 \div 10)$ mb for monopoles with $\beta = 10^{-3} \div 10^{-4}$. A $\beta = 10^{-4}$ pole would have a mean free path of 200 m in water for capture in a Mp bound state with $E_B \simeq 260$ keV, with the emission of a 260 keV photon. If a lowest-energy state exists, reaction (7) may lead to the emission of 938 MeV photons.

Monopole-nucleus bound states should exist for nuclei which have a relatively large gyromagnetic factor. Goebel [11] estimated a radiative-capture cross-section $\sigma_c \simeq 0.3$ mb for monopoles with $\beta = 10^{-3}$ in ^{27}Al nuclei. The ground state of the (M-Al) system should have a binding energy of 0.56 MeV.

The magnetic interaction between a monopole and a nucleon in a nucleus could induce some nuclear reactions, like the fission of ^{235}U.

A monopole moving with velocity v produces an electric field whose lines of force lie in a plane perpendicular to the monopole trajectory. In matter, this field may ionize or excite the nearby atoms or molecules.

The interaction with matter of poles having velocities $v > 10^{-2}c$ is well understood: a monopole with magnetic charge g behaves like an equivalent electric charge $(Ze)^2_{eq} = g^2\beta^2$. The ionization energy losses may be described by the Bohr-Bethe-Bloch formula as corrected by Ahlen et al. [11-13].

An approximate formula for poles in carbon (for $\beta > 0.04$) is

$$\left(\frac{dE}{dx}\right)_{g_D,\ ioniz} \simeq 0.72(9.0 + ln\beta^2) \quad (GeV g^{-1} cm^2) \tag{8}$$

3.2 Energy losses of slow monopoles ($10^{-4} < \beta < 10^{-2}$)

For slow particles it is important to distinguish the energy lost for ionization or excitation of atoms and molecules ("electronic energy loss") of the medium from that lost to kinetic energy of recoiling atoms or nuclei ("atomic or nuclear energy loss"). Electronic energy loss predominates the stopping power of fast electrically or magnetically charged particles for $\beta > 10^{-2}$. One must instead consider the details of the stopping medium when analyzing the energy loss of slow projectiles.

The approach adopted by Ahlen and Kinoshita [11-13] is adequate for the analysis of the electronic stopping power of GUT poles in conductors and in materials with $Z > 10$, whose electronic properties can be approximated by a Fermi gas of electrons. For the excitation of simple atoms such as hydrogen and helium, the approach of Drell et al. [10] is required.

For carbon one has the following approximation for $10^{-4} < \beta < 10^{-2}$

$$\left(\frac{dE}{dx}\right)_{g,C} \simeq 18\beta \quad (GeVg^{-1}cm^2) \tag{9a}$$

For aluminium one has for $10^{-4} < \beta < 10^{-2}$

$$\left(\frac{dE}{dx}\right)_{g,Al} \simeq (20+130)\beta \quad (GeVg^{-1}cm^2), \tag{9b}$$

where the number 20 comes from non conduction electrons and 130 from the conduction ones.

The energy loss of monopoles with $10^{-4} < \beta < 10^{-3}$ is mainly due to excitations of atoms. A monopole passing within an atom may produce substantial level mixings and crossings (Drell effect). In the $10^{-4} < \beta < 10^{-3}$ range this effect yields losses about an order of magnitude larger than ionization losses

$$in \quad H: \qquad \left(\frac{dE}{dx}\right) = 370\beta\left(1 - \frac{1.4\cdot 10^{-8}}{\beta^2}\right)^{\frac{3}{2}} \quad (GeVg^{-1}cm^2), \tag{10a}$$

$$in \quad He: \qquad \left(\frac{dE}{dx}\right) = 150\beta\left(1 - \frac{8.6\cdot 10^{-9}}{\beta^2}\right)^{\frac{3}{2}} \quad (GeVg^{-1}cm^2). \tag{10b}$$

The effect may be used for practical detection either by observing the photons emitted in the de-excitation of the excited atoms or by observing the ionization caused by the energy transfer from the excited atoms to complex molecules with a small ionization potential (Penning effect). Helium plus CH_4 or isobutane should be good working gases.

3.3. Energy losses at very low velocities ($\beta < 10^{-4}$)

Magnetic monopoles with velocities smaller than $10^{-4}c$ cannot excite atoms; they can only lose energy in elastic collisions with atoms or with nuclei. A rough estimate of the energy loss may be obtained considering the elastic interaction of a monopole with a structureless atom, characterized only by its magnetic moment. In the limit of very low velocities one has [14]

$$\left(\frac{dE}{dx}\right)_{g,Atom} \simeq N_a E_{cm}\sigma \simeq N_a \hbar^2/m_e, \tag{11}$$

where N_a is the number of $atoms/cm^3$. If $N_a \simeq 4\cdot 10^{22} atoms/cm^3$, one has $dE/dx \simeq$ 32 MeV/cm (liquid hydrogen). The results of a more precise calculation [9,14] are shown in Fig. 1. The energy is released to the medium in the form of elastic vibrations and/or infra-red radiation (thermal and acoustic energy).

For *monopole-nucleus elastic collisions* the main effect arises from the interaction of the pole magnetic charge with the magnetic moment of the nucleus, yielding

$$\left(\frac{dE}{dx}\right)_{g,nucleus} \simeq \frac{N_a \hbar^2 \mu_p}{m_p \mu_e} (\simeq 0.1 MeV/cm \quad in \quad liquid \quad H_2). \tag{12}$$

3.4. Energy losses in conductors and in superconductors.

The linear velocity dependence of the energy losses of slow monopoles in conductors seems to be well established and there is no reason to suspect the existence of a velocity threshold.

$$\left(\frac{dE}{dx}\right)_g = \frac{2\pi N_e g^2 e^2 v}{m_e c^2 v_F}\left(ln\frac{1}{Z_{min}} - \frac{1}{2}\right) \tag{13}$$

Extrapolating to superconductors, one would at first sight expect a large energy loss. However, in the region close to the pole trajectory the magnetic field would be larger than the critical field. Thus the energy loss in a superconductor should not be different from that in a normal conductor. dE/dx depends linearly on β and on the conductivity σ, and is of order of 100 $MeV\ g^{-1}cm^2$ at $\beta = 10^{-3}$.

In superconductors there is an additional energy loss. If a pole passes through a superconductor, there will be a magnetic flux $\phi_B = 2\pi\hbar c/e$ (equal to two flux quanta of superconductivity) which threads the quenched cylinder after the pole is passed, yielding $dE/dx \simeq 42$ MeV/cm. It is a small fraction of the stopping power at $\beta \simeq 10^{-3}$, but, since it is β-independent, it dominates for $\beta < 10^{-4}$.

3.5. Energy losses of monopoles in celestial bodies

For very low β ($< 10^{-4}$) poles the main energy losses in the Earth are due to i) pole-atom elastic scattering (probably velocity independent and about 20 MeV $g^{-1}cm^2$), ii) eddy current losses $dE/dx \simeq (10 \div 30)\beta$ GeV $g^{-1}cm^2$ (here the uncertainty arises from the uncertainty in the validity at low β of the formula for nonconducting electrons), iii) nuclear stopping power ($dE/dx_n \simeq 0.1$ MeV $g^{-1}cm^2$). One may conclude that the Earth should stop GUT monopoles with $\beta \leq 10^{-4}$. Similar

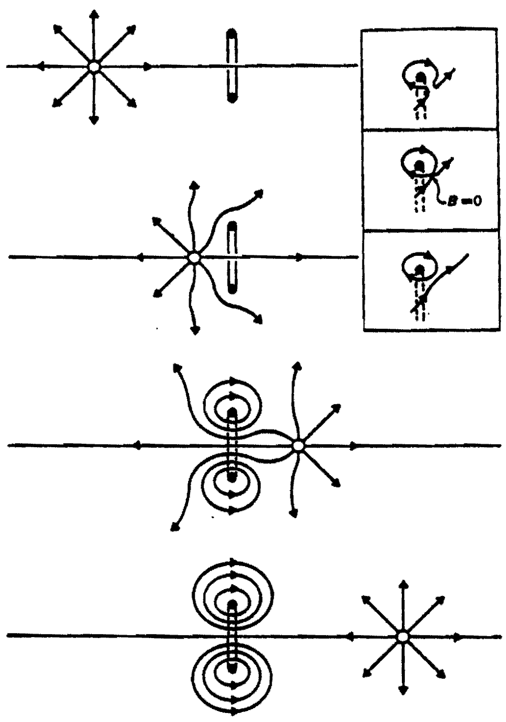

Figure 3 - Illustration of the magnetic-field lines as a monopole passes through a superconducting ring [15]. When the pole is still far away from the ring (top view), its magnetic field is the symmetric field of a point magnetic charge. As the pole approaches the superconducting ring, the field is distorted. The distortion continues when the pole passes through the ring, where it leaves some lines of force. After the passage one has the lines of force of a point magnetic charge plus the trapped lines around the coil.

estimates for other celestial bodies lead to the conclusion that poles may be stopped if they have
Moon: $\beta \leq 5 \cdot 10^{-5}$, Earth: $\beta \leq 10^{-4}$, Jupiter: $\beta \leq 3 \cdot 10^{-4}$, Sun: $\beta \leq 10^{-3}$.

4. Monopole detectors

In this Section the main techniques used in monopole search experiments are described. Probably the best technique would be that based on electromagnetic induction, i.e. the passage of a magnetic monopole in a superconducting loop. It yields a unique signature independent of monopole mass, velocity, electric charge, etc. The main drawback of this technique is that it is difficult to make large area detectors. The major techniques for monopole searches are scintillation counters, gaseous detectors and track-etch detectors.

4.1. Superconducting induction devices

The method of detection with a superconducting ring is based only on the long-range electromagnetic interaction between the magnetic charge and the macroscopic

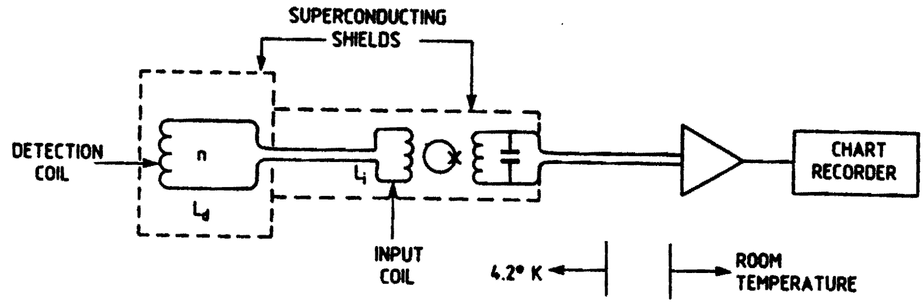

Figure 4 - Schematic diagram of a superconducting induction detector for magnetic monopoles. The detection coil is coupled to an input coil for the SQUID device, whose output is amplified and sent to a chart recorder.

quantum state of the superconducting ring. A passage of a monopole with the smallest Dirac charge and with any velocity would be observed as a jump of two flux quanta (fluxons). Induction coils are the only devices sensitive to poles of any velocity.

As already stated, a moving monopole produces an electric field; thus an electromotive force and a current (Δi) is induced when a monopole passes through a coil. For a superconducting coil with N turns and inductance L, one has (for $g = g_D$)

$$\Delta i = 4\pi N n g_D / L = 2\Delta i_o \tag{14}$$

where Δi_o is the current change corresponding to a change of one unit of the flux quantum of superconductivity, $\phi_o = \hbar c/2e$ (In practice $\Delta i \simeq 10^{-9} A$, $L \simeq$ few μH, energy $\simeq 4 \cdot 10^{-17}$ *erg*). Figure 3 illustrates the magnetic-field lines when a monopole passes through a superconducting ring [15]. The change in current will occur with a characteristic time, $b/\gamma v$, where b=radius of coil, v=velocity of the monopole and $\gamma = (1 - \beta^2)^{-1/2}$. The change in current may be observed with a magnetometer. Figure 4 illustrates the schematic layout of a superconducting induction detector. It consists of the detection coil coupled to a SQUID (Superconducting Quantum Interferometer Device). The signal from a monopole is very small and an ultrasensitive magnetic monitor such as a SQUID is needed. The detector components, in particular the magnetometer, must be well shielded from any variation of the ambient magnetic field. This places severe restrictions on the cross-sectional area of induction detectors. Variations in the ambient field may be suppressed by surrounding the detector with a superconducting shield placed inside an outer mu-metal shield.

4.2. Scintillation counters

A large number of monopole searches have been performed with ionization and excitation loss techniques. Typically, the detectors consist of multiple layers of

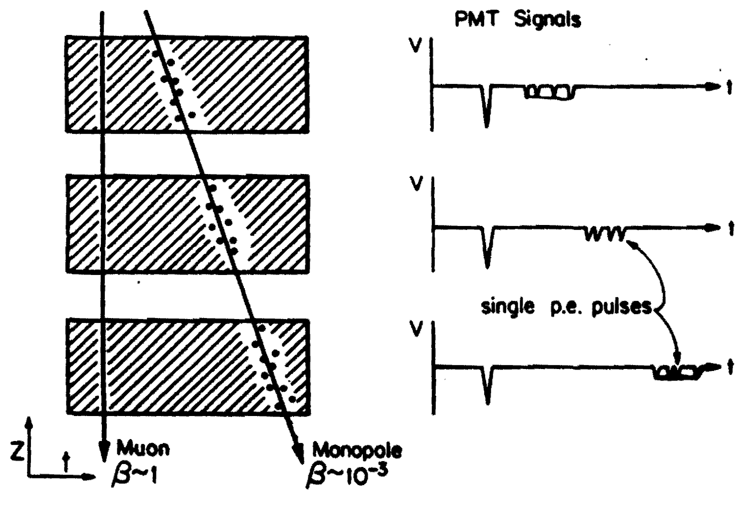

Figure 5 - A comparison of monopole and muon signals in a thick-scintillator telescope [16].

scintillators and/or gaseous detectors. The "signal" for a monopole is determined by recording the place and the time of passage in each layer, searching for slow-moving, penetrating particles, as sketched in Fig. 5 [16]. Notice the obvious importance of using waveform digitizers to detect monopoles.

Ahlen and Tarlè [13] calculated the scintillation yield of a magnetic monopole in the scintillator NE 110, Fig. 6a. Curves for a bare monopole with $g = g_D$ and for a monopole bound with a proton are given. Note the presence of a threshold at $\beta \simeq 6 \cdot 10^{-4}$, above which the light signal is large compared to that of a relativistic muon. The threshold is due to the two-body $(M - e^-)$ kinematic constraint for an energy gap of $E_G = 5$ eV. The threshold may be reduced by reducing the energy gap, for instance with acrylic-based naphtalene scintillators or with scintillators containing pentacene fluormolecules. The light yield in Fig. 6a shows the characteristic saturation effect present in solid materials at medium velocities. For $\beta > 0.1$ the light yield increases because of the production of delta rays. The light yield of Fig. 6a represents a lower limit, because any other effect should effectively lower the threshold and increase the light output. In fact direct measurements by Ficenec et al. of slow protons from $n - p$ elastic scattering in liquid scintillators prove sensivity in that material down to $\beta = 10^{-4}$, see Fig. 6b [17].

4.3. Gaseous detectors

Gaseous detectors of various types have been used: proportional chambers, Geiger tubes, proportional tubes, limited streamer tubes, etc. Here we shall only discuss the limited streamer tubes [18,19].

The mechanical structure of a typical plastic streamer tube system is shown schematically in Fig. 7a: it has a modular structure consisting of units containing 8 individual tubes. They are equipped with readouts for the wires and d pickup strips for two dimensional localization. The cross section of one 8-tube unit is shown in

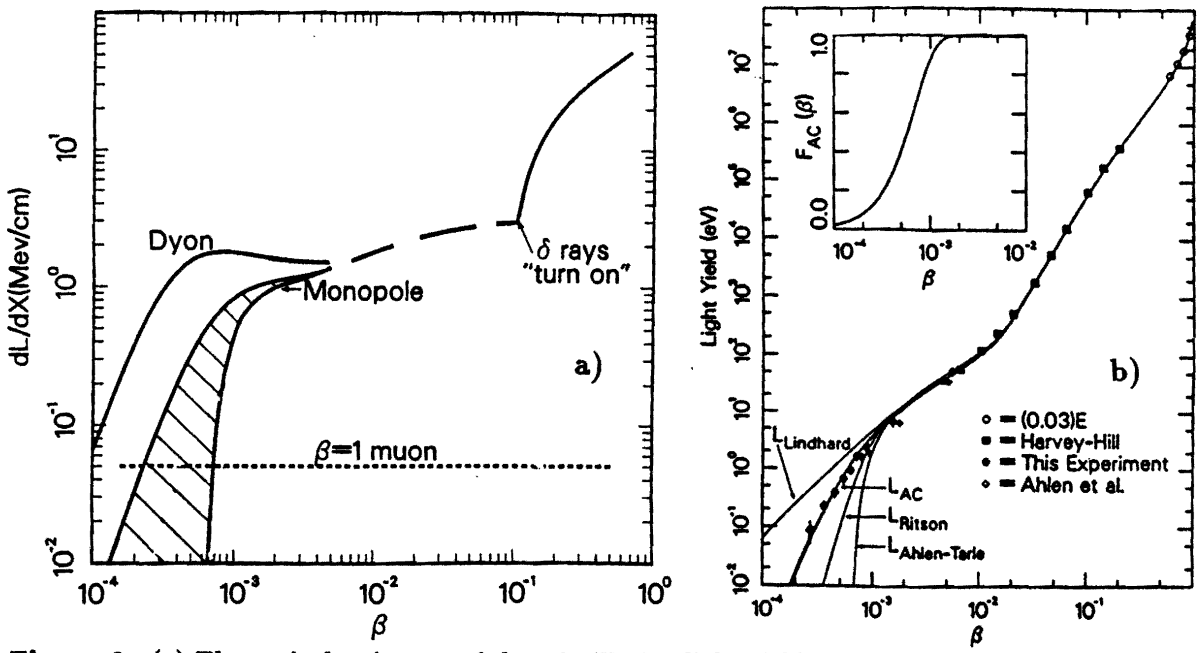

Figure 6 - (a) Theoretical estimates of the scintillation light yield in Ne 110 scintillator as a function of the magnetic-monopole velocity $\beta = v/c$ [17]. (b) Light yield in the MACRO liquid scintillators measured with recoil protons elastically scattered from a 2 keV - 24 keV neutron beams [17]: notice the sensitivity down to $\beta \simeq 10^{-4}$.

Fig. 7b. In the MACRO experiments the units are 12 m long and the single cell size is $3 \times 3\ cm^2$; the wire diameter is 100 μm. The electric field structure is of the "electrodeless" type: three sides of the cell are made conductive (with a graphite coating) and one is insulating.

If the gas used is the 3:1 mixture of argon and n-pentane, the threshold of this detector for monopoles would be $\beta \simeq 10^{-3}$. The use of helium instead of argon, allows the exploitation of the Drell+Penning effects: the passage of a magnetic monopole leaves the helium atoms in a metastable excited state (He*), with an excited energy of about 20 eV. The ionization potential of n-pentane is about 10 eV; hence, the Penning effect (collisional de-excitation and ionization) converts the energy of the He* into ionization of the n-pentane molecule. Thus the threshold becomes $\beta = 10^{-4}$, as shown in Fig. 1.

The streamer development process can be sketched as follows. When a charged particle crosses the active cell, ionization electrons from the gas drift toward the wire, where multiplication takes place as in proportional counters. Ultraviolet photons are emitted in the multiplication region; they give rise to secondary avalanches, which rapidly form a streamer orthogonal to the wire. The streamer extinguishes itself at some distance from the cathode, due to the decreasing electric field and to the quenching action of the gas mixture.

4.4. Track-etch (nuclear track) detectors

The passage of heavily ionizing particles may be permanently recorded in some insulating materials, which range from plastic sheets like CR39, lexan (makrofol E) and nitrocellulose to glasses and to minerals, like mica and obsidian. These

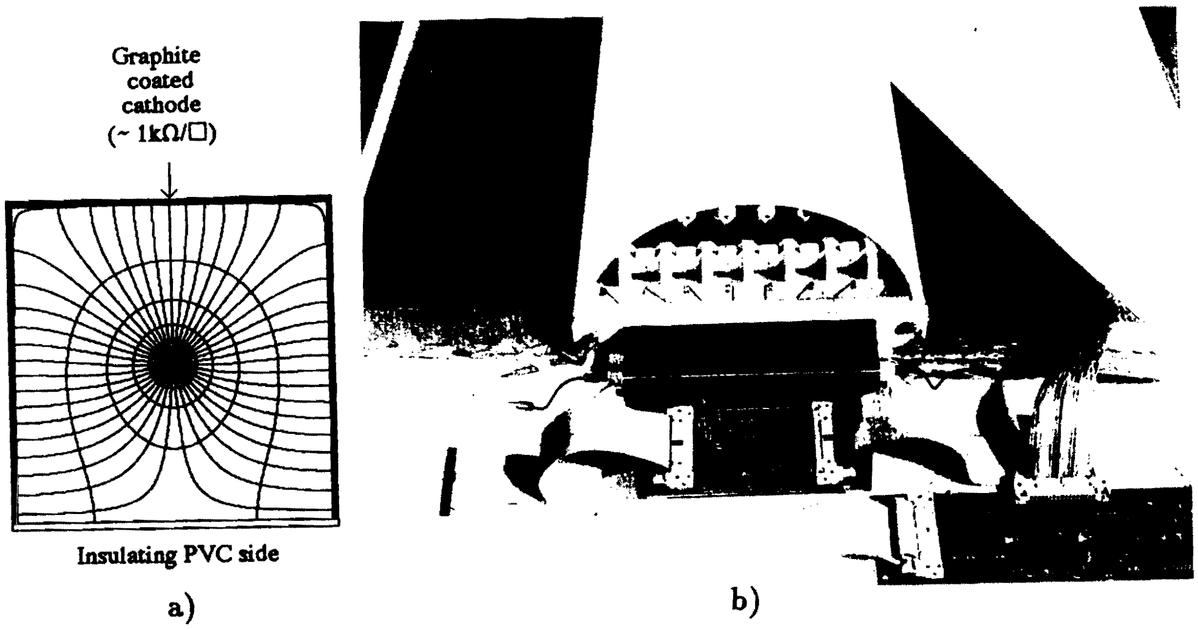

Figure 7 - (a) Sketch of a plastic streamer tube of the MACRO detector. (b) Details of an 8-cell streamer tube chamber. Two-dimensional track localization is performed by reading the wire of each tube and the d-strips placed at a stereo angle of 26.5^0 [19]. The wire and strip readout cards are also shown.

materials may be considered as threshold devices, with no time resolution and with thresholds which depend on the material and on the type of chemical etching.

The latent track may be made visible by proper chemical etching, since the etching velocity along the latent track (v_T) is greater than the bulk etch rate (v_B). Etching a layer for a short time yields two etched cones on each side of the sheet, Fig. 8b. The restricted energy loss (REL) may be determined from the geometry of the etched cones, for instance the diameter of the base of the cone. For CR39 this technique yields measurements of the electric charge of heavy nuclei to a resolution of $0.05e$, if one uses many layers, placed perpendicular to the incoming ions.

With prolonged etching one may obtain a hole in a sheet of the material (Fig. 8c). The hole may be detected by observation with low magnification-large field binoculars, or with ammonia vapour on one side of the plate: if there is a hole, the ammonia vapour passes to the other side developing a blueprint sheet [22].

Track-etch detectors are sensitive to the restricted energy loss (REL), that is to the fraction of the energy loss with δ-rays with energies smaller than 200 eV (this corresponds approximately to the energy loss concentrated in a diameter smaller than 100 Å along the direction of the primary particle). Scintillators are instead sensitive mainly to high-energy delta-rays, because of radiation quenching in the dense core region near the particle trajectory. In a certain sense a track-etch detector is complementary to a scintillator, because it is insensitive to the energy deposited in the halo and sensitive only to the energy deposited in the core (because chemical etching takes place preferentially where the density of energy deposited is large).

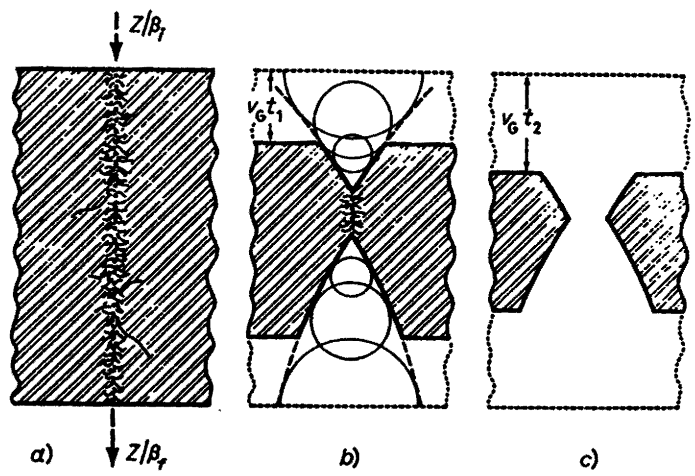

Figure 8 - Track-etching technique for particle identification: a) sketch showing the dense core of radiation-damaged material and delta-rays; b) development of conical etch pits at the inner section of the trajectory with the surface; c) development of a hole after prolonged etching [20,21].

Fig. 9 gives a schematic representation of the damage at the atomic and molecular level in a crystal and in a polymer. The response of a track-etch detector may be given as a curve of $p = v_T/v_B$ versus REL. Computed values of the restricted energy loss and of the relative etch rate for free and bound monopoles in CR39 are shown in Fig. 10.

From the above considerations and from direct measurements with heavy ions one concludes that CR39 (without DOP) has a threshold at $Z/\beta \geq 5$, which corresponds to a restricted energy loss of $\simeq$ 25 MeV $g^{-1}cm^2$. In order to compute the velocity threshold of monopoles, one has to assume a formula for their energy loss and establish the etching procedure. This may be done using the formula of Ritson [11], taking 3 eV for the effective energy gap in CR39, and considering a strong etching method. The material may be calibrated by exposure to fast and slow ions. The β-ranges to which the detectors are sensitive are the following (in parentheses are indicated more optimistic values):

CR39	$4 \times 10^{-5} < \beta < 2.5 \times 10^{-4}$, $\beta \geq 0.003$,
nitrocellulose	$\beta \geq 0.01$,
lexan	$\beta \geq 0.1$ $(\beta \geq 0.03)$,
mica	$\beta n \geq 2$ $(\beta n \geq 1.0)$,

It must be noted that there was a debate about the sensivity of the CR39 detectors to poles in the range $4 \times 10^{-5} < \beta < 2.5 \times 10^{-4}$ [23-26]. Calibrations with slow ions indicate that the MACRO and Japanese CR39 (without the DOP additive) are sensitive to this beta range [24,26].

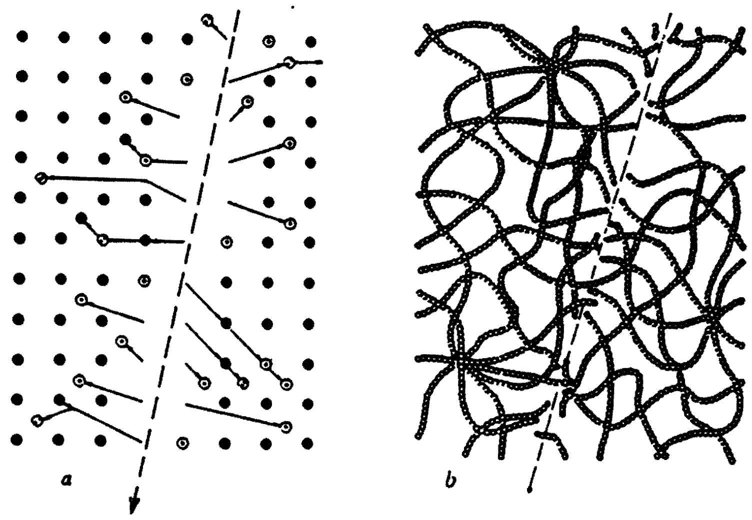

Figure 9 - Schematic representation of the damage at the atomic and molecular level produced by the passage of a heavily ionizing particle (a) in a crystal and (b) in a polymer.

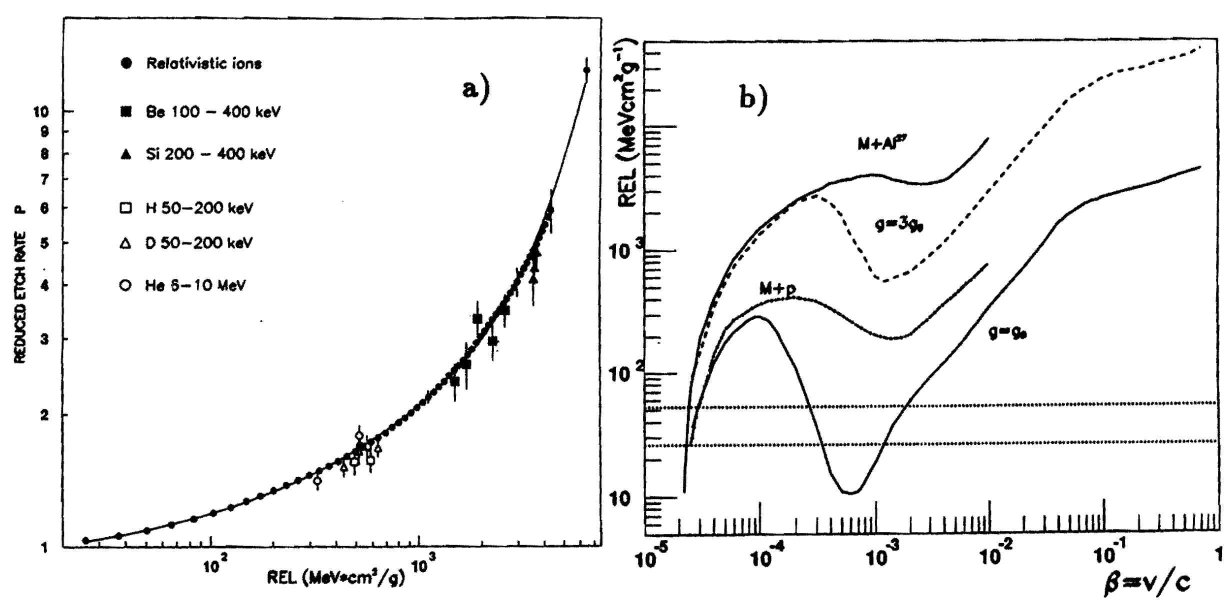

Figure 10 - (a) Calibration of CR39: Reduced etch rate $p=v_T/v_B$ versus restricted energy loss (REL). (b) Calculated values of REL vs β for free and bound monopoles in CR39 [26]. The dotted horizontal lines are the thresholds for two types of CR39 [26].

5. Searches for "classical" Dirac monopoles

In the early 1970's, the "classical Dirac" monopole was considered to be a member of the family of "well-known undiscovered objects". Experimental searches were and are made at every new higher energy accelerator.

5.1. Accelerator Searches

If monopoles could be produced at high-energy accelerators, they would be relativistic and they would ionize heavily. The experimental searches at accelerators may be classified into: i) Direct searches. ii) Indirect searches, where monopoles are searched for a long time after their production. A broad class of experiments could be classified as indirect.

Direct searches. Examples of direct searches are the early counter searches performed at the CERN Proton Synchrotron [27,28], and the experiments performed with track-etch detectors at positron-electron colliders [22,29–31], at the CERN ISR (Intersecting Storage Rings for protons) [32,33] and at the CERN and Fermilab proton-antiproton colliders [34–36]. In the experiments with track etch detectors one integrates the data over periods of months. The experiments may still be considered as direct experiments because one knows well the response of the detectors. In these experiments a set of thin plastic sheets of CR39, kapton, nitrocellulose and/or makrofol E (lexan) surrounded an intersection region. Kapton was placed inside the vacuum chamber, the other plastics outside. If magnetic monopoles were produced in e^+e^-, $\overline{p}p$ or pp collisions they should have crossed the plastic sheets, where they should have deposited a large amount of energy. After exposure, one of the sheets was "strongly" etched and scanned with one of the fast methods described in Subsection 4.4; if a signal was found, a second sheet was "lightly" etched and was later scanned with optical microscopes.

Experiments at the e^+e^- storage rings, in particular at the CERN-LEP collider, placed upper limit cross-sections of $\sim 10^{-37} cm^2$, which is considerably smaller than the QED cross-section for point particles. The experiments would exclude poles with masses up to 45 GeV. The experiments at the Fermilab $\overline{p}p$ collider, using CR39 detectors, established an upper limit of $\sim 3 \cdot 10^{-32} cm^2$ for monopoles with masses up to 850 GeV [36,37].

Indirect searches. Many indirect searches were performed at high energy accelerators [37–39]. For instance, in the experiment at the CERN SPS, the 450 GeV protons interacted (before reaching a beam dump) in a series of targets made of compacted ferromagnetic tungsten powder [39]. The poles produced in high-energy pp, pn and also πN collisions should have lost quickly their energy and be brought to rest inside the target, where they are assumed to be bound; the monopoles should have been trapped in one of the small powder pieces of ferromagnetic tungsten (this should avoid the possibility of monopole-antimonopole annihilations). Later on the targets were placed in front of a pulsed solenoid, capable of giving a magnetic field of more than 200 kG, large enough to extract and accelerate the monopoles, to be detected in nuclear emulsions and in CR39 sheets.

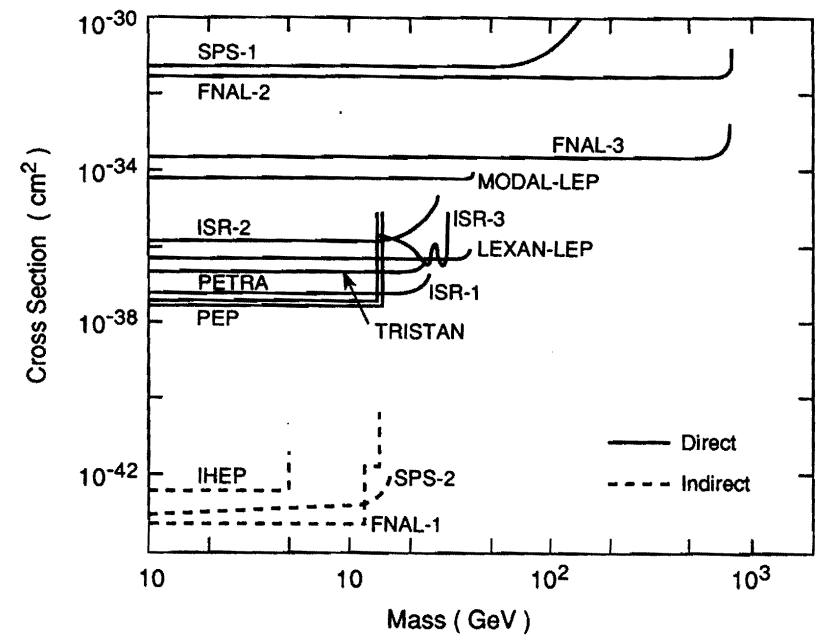

Figure 11 - Compilation of upper limits (95% C.L.) for "classical" magnetic monopole production obtained at high-energy accelerators plotted vs. monopole mass. Solid and dashed lines refer to "direct" and "indirect" measurements (see text).

In these indirect experiments one can in principle obtain very good cross-section upper limits, because of intense beams and because one can integrate over long time intervals.

But there are many hypotheses on the behaviour of monopoles in matter: each experimental group took special precautions to avoid possible pitfalls; examples of these precautions are the above mentioned segmentation of the targets, the use of stripper foils before acceleration (in order to dislodge the paramagnetic molecules which may attach to a monopole), etc.

Figure 11 summarizes schematically, as a function of the monopole mass, the production cross-section upper limits (at the 95% $C.L.$) in pN, $\bar{p}p$ and e^+e^- collisions. Figure 12 summarizes the same limits as a function of the monopole magnetic charge. Solid lines refer to "direct" measurements, dashed lines to "indirect" measurements at high-energy accelerators. Table 1 gives a summary of the recent searches at the highest-energy accelerators.

Multi-γ events. Five peculiar photon shower events were found in nuclear plates exposed to high-altitude cosmic rays [40]. The five events are characterized by a very energetic narrow cone of tens of photons, without any incident charged particle. The total energy in the photons is of the order of 10^{11} GeV. The radial spread of photons ($10^{-3} \div 10^{-4}$ rad) suggests a c.m. velocity corresponding to $\gamma > 10^3$. The energies of the photons in the overall c.m. system are very small, orders of magnitude too low to have π^0 decays as their source. One of the possible explanations of these events could be the following: a high-energy γ-ray, with energy larger than 10^{12}eV, produces in the plate a pole-antipole pair, which then suffers bremsstrahlung and annihilation producing the final multi-γ events.

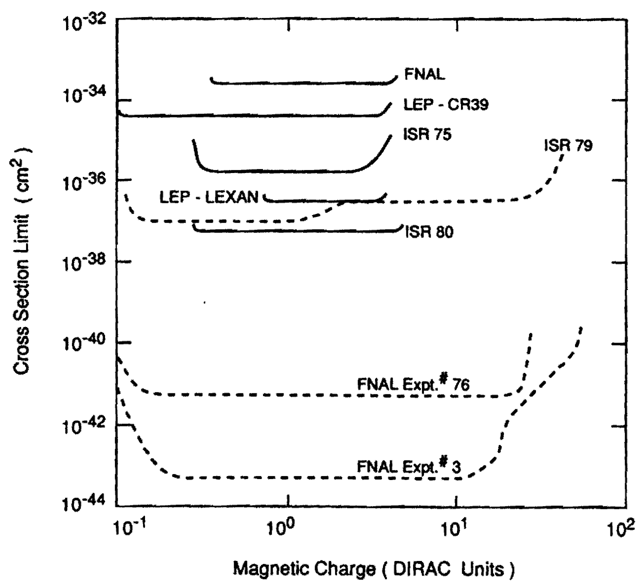

Figure 12 - Compilation of upper limits (95% C.L.) for classical-monopole production versus magnetic charge. Solid and dashed lines refer to "direct" and "indirect" measurements (see text).

Table 1 - Recent experimental searches for "classical Dirac monopoles" at the highest-energy accelerators. The cross section limits are at the 95% C.L.

Accelerator	Collision	$\sqrt{s}$ (GeV)	Technique	Mass (GeV)	Magnetic charge (g_D)	Cross-sect limit (cm^2)	Ref.
PEP	e^+e^-	29	CR39	< 14	$0.5 \div 3$	10^{-37}	22
PETRA	e^+e^-	40	kapton	< 20	$0.8 \div 3$	$5 \cdot 10^{-38}$	30
SPS	pN	28	W-grains	< 14	$0.1 \div 20$	10^{-43}	39
SPS coll.	$\bar{p}p$	540	kapton	< 150	$0.8 \div 3$	10^{-32}	34
Tristan	e^+e	52	CR39, VG5	< 24	$0.5 \div 2$	$8 \cdot 10^{-37}$	29
Fermilab	$\bar{p}p$	1800	CR39, BP1	< 850	$0.5 \div 3$	$1.2 \cdot 10^{-33}$	35
Fermilab	$\bar{p}p$	1800	CR39	< 850	$0.5 \div 3$	$2 \cdot 10^{-34}$	36
LEP	e^+e^-	91	CR39	< 45	$0.1 \div 3.6$	$7 \cdot 10^{-35}$	29
LEP	e^+e^-	91	lexan	< 45	$0.9 \div 3.6$	$3 \cdot 10^{-37}$	31

Accelerator experiments performed at the ISR, at Fermilab and at LEP failed to observe these multigamma events [11,41–43]. The ISR experiment, at a center of mass energy of 53 GeV, placed an upper-limit cross-section of $10^{-37} cm^2$.

5.2. Searches in bulk matter

Several searches for magnetic monopoles trapped in bulk matter have been performed. In order to have a sensitive search, one has to establish where monopoles would stop, where they would be trapped and then device a method of detection. Classical monopoles could be produced by cosmic rays and should have relatively low kinetic energies. Thus they could stop at the surface of the Earth (or of the Moon), where they could be trapped in ferromagnetic (paramagnetic) materials. It is instead improbable that GUT poles would stop close to the surface of the Earth.

A search was performed with lunar rocks; one has to remember that the lunar material was taken to the Earth, experiencing high decelerations, hundred times the acceleration of gravity at the earth surface. Monopoles trapped in all materials, but ferromagnetic, would have been lost.

Searches were made using meteorites. Since all elements heavier than hydrogen and helium were synthesized inside stars and thrown into space in stellar explosions, it is unlikely that meteorites would originally be very rich in monopoles. They would have to pick up monopoles in their travel. Furthermore, monopoles in meteorites may get lost when they impact the Earth, since they experience decelerations of $\simeq 10^3$ times the acceleration of gravity on the earth surface; moreover, parts of the meteorites melt.

Samples of terrestrial, lunar and meteoritic materials were passed through a superconducting loop, or placed in a high-field pulsed magnet, which would extract and accelerate the poles; the detectors were nuclear emulsions or counters. An experiment used as detector a superconducting coil in which an electric field, and thus a current change, would be induced by a magnetically charged particle present in a sample which was moved through the coil [44]. Using multiple traversals of the sample, the proper sensitivity was achieved. Samples of 20 kg of lunar material, several kilograms of magnetite from earth mines and 2 kg of meteorites were used. The authors placed a limit of less than $2{\cdot}10^{-4}$ monopoles per gram of lunar material. Assuming a constant monopole flux over the long time during which the Moon remained unaltered, they estimated a pole flux $F < 8 \cdot 10^{-18}$ poles $cm^{-2}s^{-1}sr^{-1}$. This flux limit applies to poles of small mass, it becomes less significant for poles with higher kinetic energies and it is irrelevant for kinetic energies larger than 10^8 GeV. Assuming instead that monopoles could be produced by cosmic rays, the cross-section upper limits were at the level of $10^{-39} cm^2$ for poles with a mass of 30 GeV.

Another group searched for monopoles in magnetite (from a surface mine), from ferromanganese nodules (from deep ocean sediments) and from sea water [45,46]. The poles should have been extracted, accelerated and sent towards a detector by a large magnetic field (pulsed or continuous). The detectors consisted of plastic sheets of lexan and nitrocellulose. While the field was sufficient to extract all poles, it would provide poles with sufficient velocities to produce ionization only if the pole masses were smaller than 10^4 GeV. The experiment used 7.7 kg of material, having an age of approximately 16 million years. The authors estimated that this corresponds to a flux $F < 10^{-19} cm^{-2} s^{-1} sr^{-1}$ if the poles were stopped at the surface of the Earth.

5.3. Searches in the cosmic radiation

Searches for a flux F of classical fast monopoles were made in the '60s and '70s using counters, track-etch detectors and nuclear emulsions. One assumed that poles could have been produced in the upper atmosphere by energetic cosmic rays. The experimental upper limits were modest, $F < 7 \cdot 10^{-11} cm^{-2} s^{-1} sr^{-1}$.

Some of these searches, made with electronic detectors, were aimed at detecting lowly ionizing quarks at sea-level and at mountain altitude. The information on magnetic poles was only indirect based on a reanalysis of the data.

In 1975 a monopole candidate from a high altitude, balloon-borne stack of nuclear track detectors, nuclear emulsions and a Cherenkov detector was reported [20]. The detector had an area of $18m^2$, was quite elaborate (35 layers of lexan and 3 of nuclear emulsion) and was flown for 15 days. The main purpose of the experiment was the search for heavy nuclei in the cosmic radiation. After a long debate the authors concluded that they had an unusual event, which could be: i) a supermassive particle with $\beta \simeq 0.4$, $z \simeq 95$ and $m > 10^3$ GeV; ii) a fast antinucleus with $z/\beta \simeq -110$, $76 \leq z < 96$; the antinucleus fragmented and lost one or two charges; iii) a fast nucleus with $z \simeq 112$, $\beta \geq 0.99$. Because of inconsistencies in the various detector readings, the authors excluded a monopole, and added that the event could also be compatible with a monopole with $\beta \simeq 0.4$, $n = 2$, $m > 10^{11}$ GeV; they said that "such a large mass is not excluded by theory; but is perhaps offensive". From this exposure and from subsequent ones [47] one had $F < 2 \cdot 10^{-13} cm^{-2} s^{-1} sr^{-1}$.

Searches were made for ancient tracks in mica and obsidian. As stated in Subsect. 4.5, mica and obsidian are track-etch detectors with high thresholds. Within this limitation, flux upper limits of $F < 10^{-19} cm^{-2} s^{-1} sr^{-1}$ in mica and $F < 3 \cdot 10^{-18}\ cm^{-2} s^{-1} sr^{-1}$ in obsidian were reported. The limits will be discussed in Subsect. 7.3.

In conclusion, most of the searches for classical monopoles performed until 1981 were not relevant to the question of the existence of very massive poles [4,5,7,8,48,49]. Ruzicka and Zrelov made a summary of all types of searches for classical monopoles performed before 1981 [4,50].

6. Cosmological and astrophysical bounds on GUT poles

Upper limits for a GUT monopole flux in the cosmic radiation were obtained on the basis of cosmological and astrophysical considerations. Most of the bounds must be considered as rough orders of magnitude only since many loopholes may be present in many astrophysical considerations.

6.1. Limit from the mass density of the Universe

This cosmological bound may be obtained requiring that the present monopole mass density be smaller than the critical density ρ_c of the Universe, that is the minimum density which would close the Universe. In terms of the Hubble constant H_0 and of the gravitational constant G_N the critical mass density is given by

$$\rho_c = \frac{3H_0^2}{8\pi G_N} \simeq 1.9 \cdot 10^{-29} h_0^2 \simeq 1.1 \cdot 10^{-29} \; (g\ cm^{-3}), \tag{15}$$

where h_0, with $0.5 < h_0 < 1$, expresses our ignorance on the Hubble constant H_0; for numerical estimates the value $h_0 = 0.75$ may be used. From $\rho_M = n_M m_M < \rho_c$ (n_M is the monopole number density) and $F = n_M v_M / 4\pi$, one has the following limit of the monopole flux F for $m_M = 10^{17}$ GeV:

$$F = \frac{n_M c}{4\pi}\beta < 3 \cdot 10^{-12} h_0^2 \beta \; (cm^{-2} s^{-1} sr^{-1}). \tag{16}$$

This limit is valid for poles uniformly distributed in the Universe. If poles are clustered in galaxies the flux limit is 4-5 orders of magnitude greater.

6.2. Limit from the magnetic galactic field. The Parker limit

Most celestial bodies possess large-scale magnetic fields. The magnetic field in our Galaxy is stretched in the azimuthal direction along the spiral arms, and is very probably due to the non-uniform rotation of the Galaxy. This mechanism generates a magnetic field with a time scale approximately equal to the rotation period of the Galaxy ($\tau \sim 10^8\ yr$). Since magnetic poles are accelerated in magnetic fields, they would gain energy, which is taken from the stored magnetic energy. An upper bound for the monopole flux may be obtained be requiring that the kinetic energy gained per unit time by magnetic poles be equal to or smaller than the magnetic energy generated by the dynamo effect. This yields the so called Parker limit. The original limit [51], $F < 10^{-15}\ cm^{-2} s^{-1} sr^{-1}$, was reexamined to take into account the almost chaotic nature of the galactic magnetic field (with coherent lengths of about $\ell \sim 1\ kpc$); the limit was shown to be mass dependent [52]. For $m_M = 10^{17}$ GeV the limit is:

$$\begin{aligned} &\text{for} \;\; \beta \le \beta_c \simeq 3 \cdot 10^{-3}: \quad && F_G \le 10^{-15}\ cm^{-2} s^{-1} sr^{-1}; \\ &\text{for} \;\; \beta > \beta_c \simeq 3 \cdot 10^{-3}: \quad && F_G \le 10^{-15} (\beta/\beta_c)^2\ cm^{-2} s^{-1} sr^{-1}. \end{aligned} \tag{17}$$

The limit could be more stringent if one assumes that some of the monopole energy could be given back to the galactic field when poles encounter regions where they are decelerated.

Recently an extended Parker bound was obtained by considering the survival of an early seed field [53]. The result is:

$$F \le 1.5 \cdot 10^{-16} (m_M / 10^{17} GeV)\ cm^{-2} s^{-1} sr^{-1} \tag{18}$$

6.3. Limit from the intergalactic field

Raphaeli and Turner [54] assumed the existence in the local group of galaxies of an intercluster field $B_{IC} \sim 3 \cdot 10^{-8}\ G$ with a regeneration time $\tau_{IC} \sim 10^9\ y$.

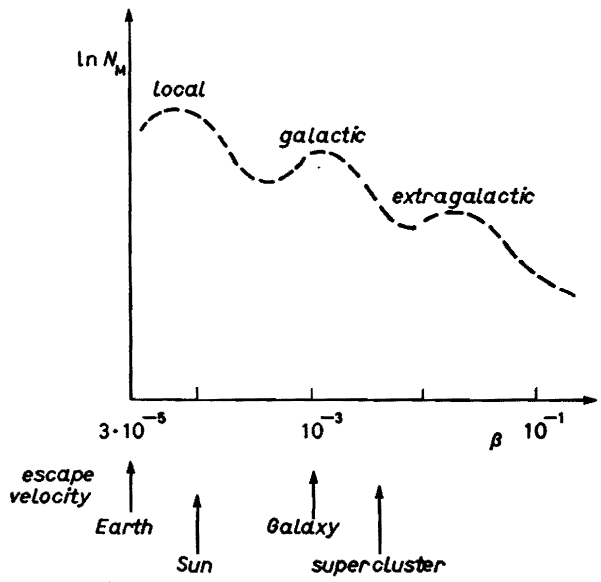

Figure 13 - Sketch of a possible velocity spectrum of GUT monopoles with 10^{17} GeV mass arriving on Earth. The various peaks correspond to poles bound locally, bound to the Galaxy and to the extragalactic flux. Notice that the vertical scale is arbitrary. In the horizontal scale the escape velocities from various astrophysical systems are indicated.

Applying the same reasoning discussed in the previous section, they obtained a flux limit about three orders of magnitude more stringent than the Parker bound; but the limit is less reliable because the knowledge of the existence and of the persistence of the intergalactic field are not well established.

6.4. Limits from peculiar A4 stars and from pulsars

Peculiar A4 stars have their magnetic fields ($B \sim 10^3$ G) in the direction opposite to that expected from their rotation. This may be explained assuming that the fields have been "frozen in" at the formation time of the stars, estimated for some stars to be $t_s \sim 5 \cdot 10^8$ yr ago.

A typical galactic monopole with $\beta \sim 10^{-3}$ should lose enough energy when traversing an A4 star to be stopped: thus the number of monopoles in the star will increase with time (neglecting $M\overline{M}$ annihilation inside the star). The poles would be accelerated in the magnetic field, which should, therefore, decrease with increasing time. Repeating the Parker argument, assuming a typical time of 5×10^8 yr to regenerate the magnetic field, one obtains a limit for the monopole density [55]. The monopole velocity is now a drift velocity, which may be estimated equating the rate of energy loss of the monopole in the star to the rate of energy gained in the magnetic field. One obtains

$$F = \frac{n_M R_s}{3t_s} < 3 \cdot 10^{-20} cm^{-2} s^{-1} sr^{-1} \tag{19}$$

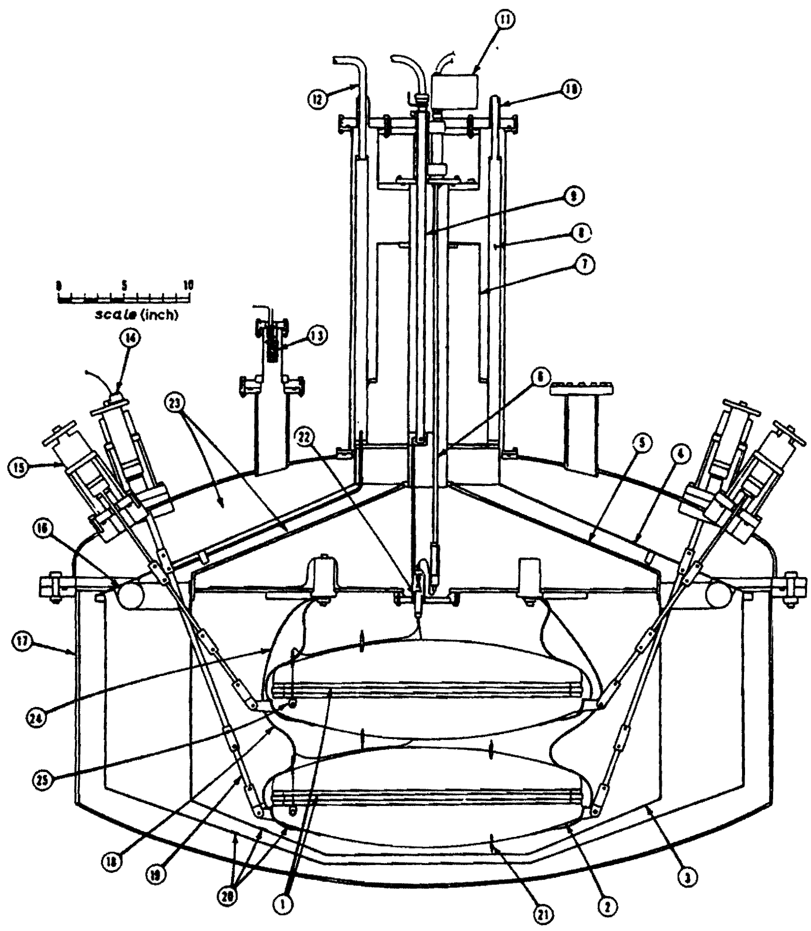

Figure 14 - Sketch of the Chicago superconducting detector [58].

using $R_s = 10^{11}$ cm. This limit should apply to the flux of poles with $\beta < 3 \cdot 10^{-3}$, since faster poles would pass through the star without stopping. It is a strong limit, but it is not clear how good are all the assumptions. In fact, as already stated, most astrophysical limits have loopholes and uncertainties.

With similar considerations on the superconducting core of neutron stars, the field survival of a pulsar gives an upper limit of monopole flux in the neighborhood of the pulsar. The limit is particulary stringent for pulsar PSR 1937+214.

6.5. Other limits

Other limits have been obtained for monopoles trapped by the Earth, from the magnetic field structure (absence of a monopole term) of the Earth, Sun and other celestial bodies [5]. Limits arising from the possible catalysis of proton decay by monopoles will be discussed in Section 8.1. Also for all these limits are valid, and even more so, the words of caution expressed in Subsection 6.4.

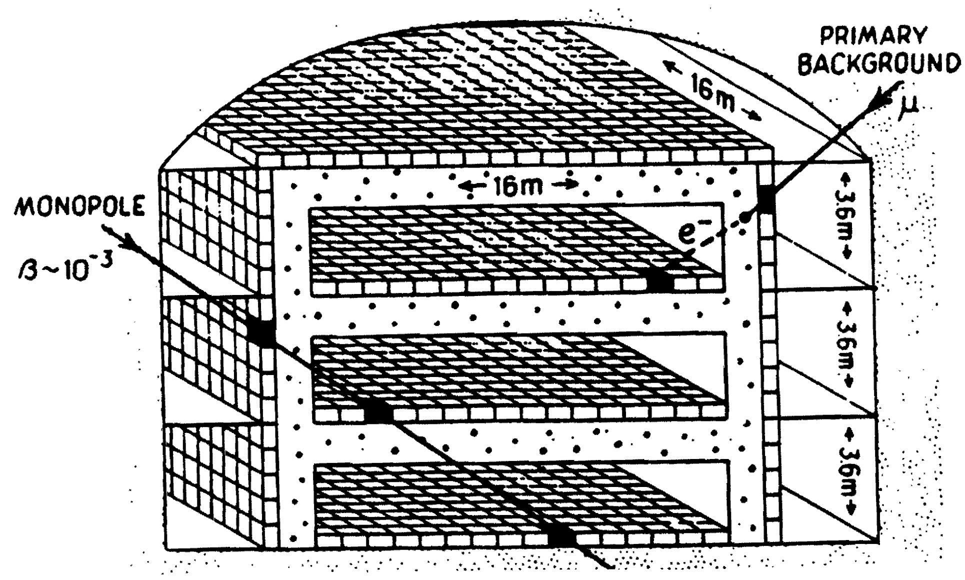

Figure 15 - Layout of the Baksan liquid-scintillator detector [65].

7. Searches for GUT poles

A flux of cosmic GUT monopoles may reach the Earth and may have done so for the whole life of the Earth. A falling pole with zero initial velocity would reach a velocity equal to the escape velocity from the Earth ($\beta \simeq 3.7 \times 10^{-5}$). The velocity spectrum of the monopoles hitting the Earth could be of the type shown in Fig. 13, from which one concludes that $3 \cdot 10^{-5} < \beta < 0.1$ may be the experimentally interesting range for searches of GUT poles with mass $\sim 10^{17}$ GeV. GUT monopoles with an intermediate mass (for instance 10^{10} GeV) could be relativistic. Therefore it is advisable that experiments be sensitive also to higher velocities.

Searches for cosmic poles may be classified as i) direct searches for a flux of poles reaching now the Earth, ii) searches for tracks left in certain materials over the ages by passing poles, iii) searches for poles which over the ages have been trapped in earth ferromagnetic materials; iv) the detection via catalysis of proton decay is considered in the next Section.

The searches for GUT poles do not differ in principle from the searches for classical poles, but there are differences arising mainly from the low speed and large mass of the cosmic monopoles.

Initial experiments performed in late 1970's and early 1980's were small-scale experiments, some of those being of the "quick and dirty" type. Later on, detectors specifically designed for low pole velocities and large underground proton-decay detectors were used. Now, only few large underground detectors are in use.

In the following we shall discuss the searches performed with superconducting induction coils, with electronic detectors, with track-etch detectors and bulk matter searches. The most relevant parameters of the first searches are the geometrical acceptance (effective area S times the solid angle Ω) and the range of monopole velocities (β-range) to which the experiment is sensitive.

7.1. Searches with superconducting induction devices

In 1982 a Stanford group successfully operated a four-turn coil of 5 cm diameter [6]. In the first 151 days of operation they recorded a single current jump corresponding to that expected from a monopole with $g = g_D$ (The author stated that "although a spontaneous and large mechanical impulse seems highly unlikely in an unoccupied laboratory, the evidence presented by this single event does not preclude that possibility"). No other jump was observed in subsequent runs. This candidate event generated a great deal of interest in induction detection of monopoles. The technique evolved quickly and several groups later operated second-generation experiments, characterized by large areas (each cell is small), coincidence arrangements and sophisticated procedures for eliminating the background [56]. The Chicago detector is shown, in Fig. 14, as an example of these detectors.

The Stanford event was not confirmed, though the Imperial College experiment [62] had some unexplained candidates.

Table 2 summarizes the experiments with superconducting induction devices, their main features and the upper limits obtained. The global upper limit may now be placed at $F < 2 \cdot 10^{-14} cm^{-2} s^{-1} sr^{-1}$. This limit is also shown in Fig. 19.

Table 2 - Searches for cosmic GUT monopoles with superconducting induction devices. The table gives for each group the main feature of the apparatus, the effective area for which one has a 4π solid angle and the flux upper limit (90% confidence level; the value in the first line corresponds to one event). The overall combined upper limit is presently about $2 \cdot 10^{-14} cm^{-2} s^{-1} sr^{-1}$.

Group	Main feature	Physical area (cm^2)	Area/4π ($cm^2/4\pi$)	Flux limit ($10^{-12} cm^{-2}$ $s^{-1} sr^{-1}$)	Reference
Stanford 1	single coil	20	10	610	4
Stanford 2	3 coils	79	71(476)	4.4	57
Stanford 3	8 coils	8800$\times$ 8	15000	0.72	57
CFM*	2 coil grad.$^+$	9500	4400	7.1	58
IBM-1	2 coil grad.	100	25	510(170)**	59
IBM-2	6 coil grad.	4000	1000	5.5	60
Kobe	single coil	50-300	25	140	61
IC	2 coils	1120	1800	1.5	62
NBS	3 coils	–	1195	5.0	63

(*) Chicago-FNAL-Michigan
(**) Using also non-coincident recordings.
(+) Gradiometers.

Table 3 - Summary of monopole searches using relatively small scintillator layouts [8,64,65] The dE/dx is relative to minimum ionizing particles.

Experiment	$S\Omega$ ($m^2 sr$)	(dE/dx) (min.ion.)	β-Range	Flux Limit ($10^{-13} cm^{-2} s^{-1} sr^{-1}$)
Bologna	10-36	10-20	$10^{-3} - 0.6$	3
Tokyo	1.4	0.2	$3 \cdot 10^{-4} - 5 \cdot 10^{-3}$	150
Tokyo-Kam.	22.0	0.05	$6 \cdot 10^{-4} - 5 \cdot 10^{-3}$	15
Tokyo-ICRR	11.0	0.05	$4 \cdot 10^{-4} - 10^{-2}$	810
Utah-Stanf.	2.7	0.13	$> 2 \cdot 10^{-3}$	81
BNL ν-expt.	14.5	0.3	$10^{-3} - 0.2$	52
Berk.-Indiana	17.5	0.3	$6 \cdot 10^{-4} - 2 \cdot 10^{-3}$	4
Kobe	20.0	0.1	$3 \cdot 10^{-3} - 0.2$	50
Texas A.M.	262-400	0.1	$8 \cdot 10^{-4} - 0.1$	0.3
Mont Blanc-2	700	0.2	$4 \cdot 10^{-3} - 10^{-2}$	
Caltech	6.7	0.33	$3 \cdot 10^{-4} - 5 \cdot 10^{-3}$	47

Table 4 - Summary of monopole searches using gaseous detectors [8,66].

Experiment	Detec. Mode	*Gas Mix.*	$S\Omega$ ($m^2 sr$)	β−Range	Flux Limit ($10^{-13} cm^{-2} s^{-1} sr^{-1}$)
BNL	Prop.	Ar, CH_4	1.9	$3 - 12 \cdot 10^{-4}$	340
KGF	Prop.	Ar, CH_4	250	> 0.0012	0.03
M. Blanc 1	Strea.	Ar, CO_2, C_5H_{10}	19	> 0.02	5
Soudan I	Prop.	Ar, CO_2	72	$0.002 - 0.01$	1
Tokyo-ICRR	Prop.	He, CH_4	24.7	$3 \cdot 10^{-4} - 1$	7
San Diego	Prop.	He, CH_2	32.4	$> 10^{-4}$	0.2
Frejus	Geig.	Ar, CH_2	880	$0.0008 - 0.1$	0.5
Akeno	Prop.	He, CH_4	130	$0.0007 - 1$	1.2

7.2. Searches with scintillators and gaseous detectors

The simplest layout of an electronic system designed to detect a flux of cosmic GUT poles consists of two-three counters, which measure the energy loss and the times of flight. Larger area layouts consist of hodoscopes, arranged in several layers, often employing different types of electronics detectors. Table 3 summarizes the relatively small experiments using scintillation counters [8,64], while Table 4 summarizes those using gaseous detectors [8,65]. The tables give some relevant parameters, like the values $S\Omega$=area times solid angle, the minimum dE/dx detected, the β-range covered and the flux limit obtained.

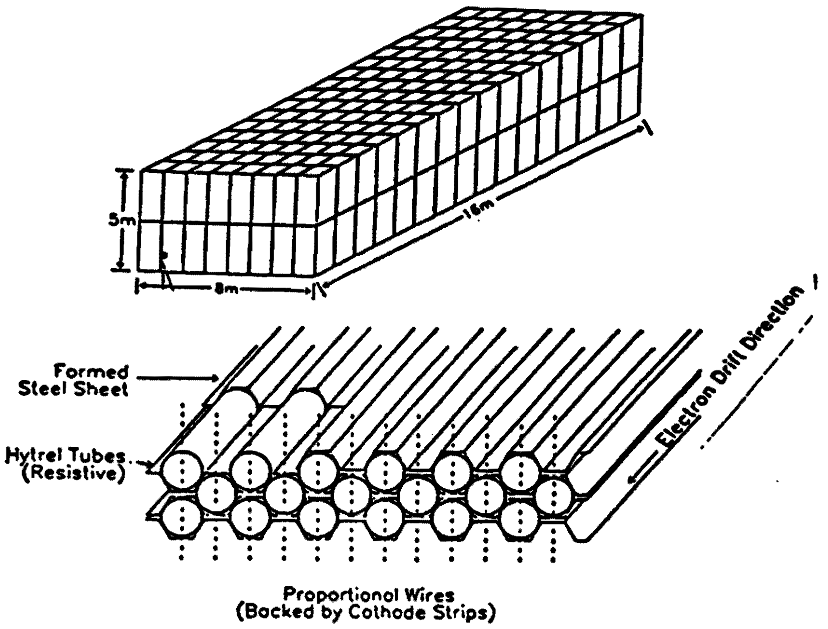

Figure 16 - Layout of the Soudan 2 detector [67].

Cosmic rays are a large background for large area detectors. It thus becomes necessary to install them in underground laboratories, where the muon flux is of the order of one million times smaller than at the surface. Here follows a brief list of large underground detectors with some of their main features.

The Baksan experiment [65], in Russia, uses the neutrino liquid scintillator telescope, see Table 7 and Fig. 15. For monopole search, the energy loss threshold is set at 0.25 I_{min}. I_{min} is the minimum ionizing value of about 1.5 MeV/cm. A flux limit of $0.4 \cdot 10^{-15} cm^{-2} s^{-1} sr^{-1}$ was reported for poles with $10^{-3} < \beta < 0.5$ [64].

The nucleon decay experiment Soudan-2 [67], located in the Soudan mine in the U.S., uses modules with proportional tubes. It has $S\Omega \simeq 3000\, m^2 sr$. For monopoles, the detector is set to cover the range $\beta > 10^{-3}$, see Table 6 and Fig. 16 [65].

One Tokyo group used a stack of scintillation counters and of proportional chambers, employing 90% gaseous helium and 10% CH_4 (see Table 4). In the proportional chambers the monopoles may excite helium atoms via the Drell mechanism $He \xrightarrow[pole]{} He^*$. Then, by the Penning effect, the excitation energy of the excited He^* is transferred into ionization of the CH_4 molecule, $He^* + CH_4 \rightarrow He + CH_4^+ + e^-$. Therefore, one may obtain an effective ionization also for low-velocity monopoles in the $10^{-4} < \beta < 10^{-2}$ range. The San Diego detector followed the same approach (see Table 4).

The proton decay experiment in the Frejus tunnel [68], between France and Italy, was a fine-grain calorimeter of $(6 \times 6 \times 13)\ m^3$ dimension and weight $\simeq 1000t$ (see Table 4). It was made of 1000 flash-tube planes interspersed with two 1.5 mm iron plates; 120 Geiger tube planes were used as trigger. As a monopole detector, it could detect poles with few $10^{-3} < \beta < 0.1$; it had $S\Omega \simeq 880 m^2 sr$ and reached a flux limit of $5 \times 10^{-14} cm^{-2} s^{-1} sr^{-1}$ [66].

The KGF proton decay experiments [69] in the Kolar gold mine in India was a calorimeter with total area 60 m^2 and weight 260 t.

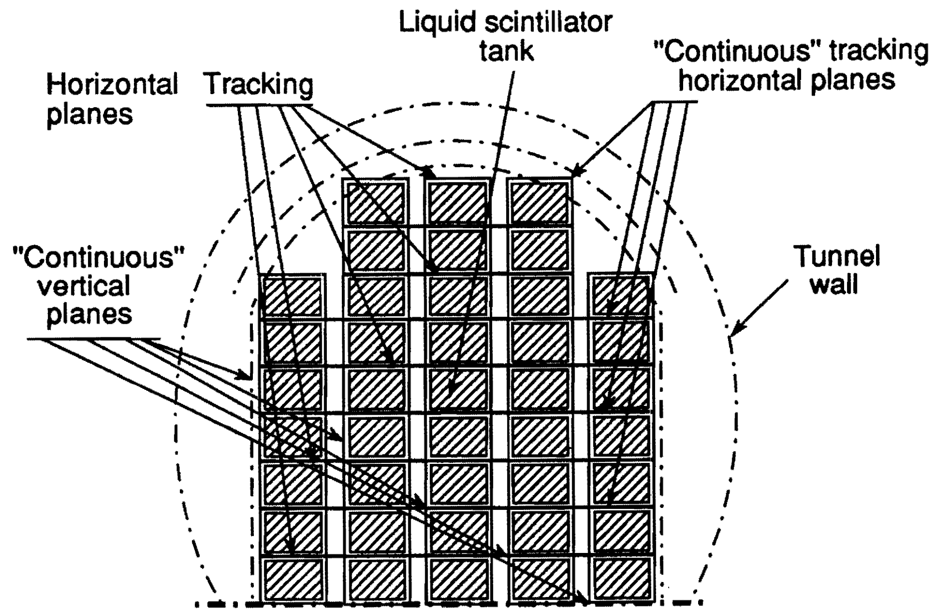

Figure 17 - Layout of the LVD experiment at Gran Sasso [70].

7.3. Searches with Track-etch detectors

As already stated, track-etch detectors record the passage of charged particles by submicroscopic damage trails in the lattice of the detector material. These trails can be amplified and made visible by chemical etching. For each detector, there is a well defined response function for the rate at which etch pits develop versus z/β. A summary of direct experiments which used the track-etch technique to search for GUT monopoles is given in Table 5; the large layouts are described in Table 7.

Table 5 - Summary of direct monopole searches using track-etch detectors [8,70].

Exper.	Detector	S (m^2)	$S\Omega$ ($m^2 sr$)	β-Range	Flux limit ($10^{-13}cm^{-2}s^{-1}sr^{-1}$)
Berkeley	CR-39	-	150	0.02-1	1.5
Kitami	nitrocellulose	-	1000	0.04-1	0.052
Norikura	CR39	200	-	0.02-1	
Kamioka	CR39	160	-	> 0.01	0.04
Kamioka	CR39	2000	-	see Fig. 19	see Fig. 19
MACRO	CR39	1200	-	see Fig. 19	see Fig. 19

Some indirect searches used ancient mica as nuclear track detectors [72,73]. If a monopole captures a heavy nucleus, then mica could be sensitive to monopoles with velocity around $10^{-4}c$, provided that the nucleus is at least as heavy as aluminium. The mica experiment scenario assumes that a bare monopole passing through the

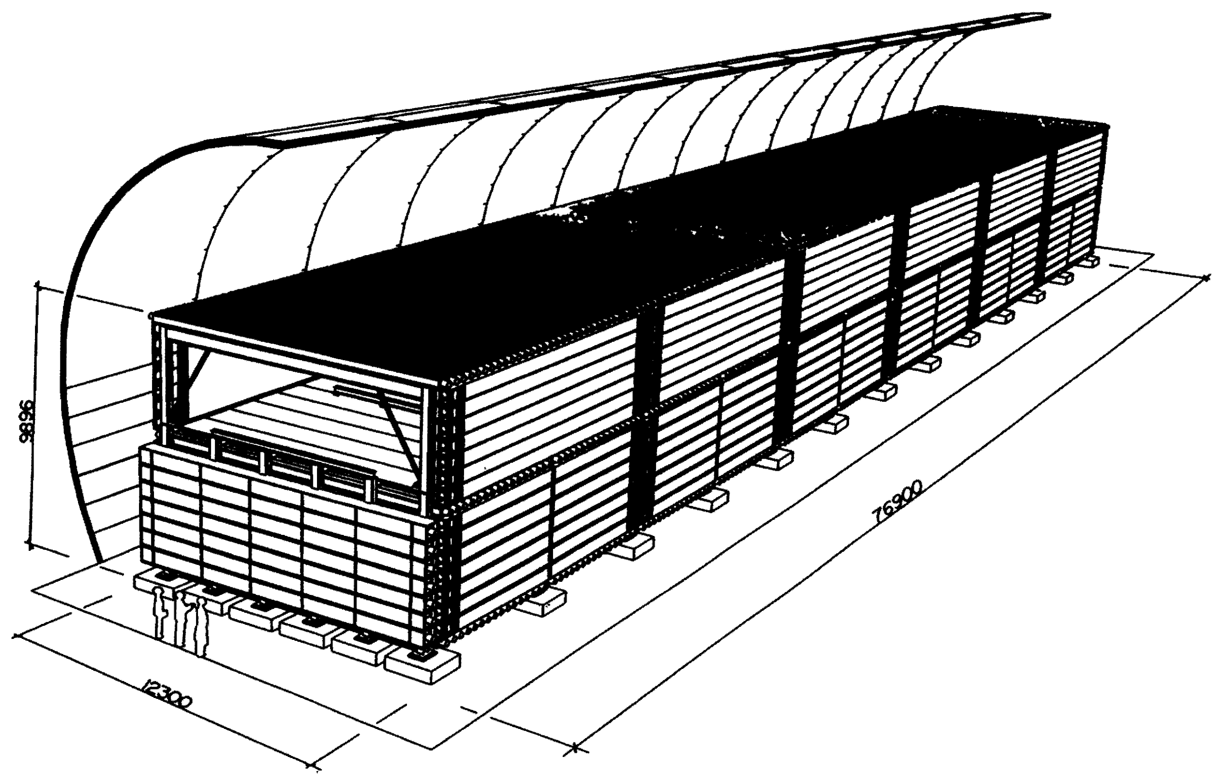

Figure 18 - Layout of the MACRO experiment in Hall B of the Gran Sasso Laboratory [71].

Earth captures an aluminium nucleus and drags it through subterranean mica causing a trail of lattice defects. As long as the mica is not reheated, the damage trail will survive. The pieces of mica analyzed by the Berkeley-Indiana [72] and the Calcutta [73] experiments are small (13.5 cm^2 and 18 cm^2, respectively), but have been recording tracks since they cooled 4.6×10^8 and 9×10^8 years ago. They can thus quote upper limit fluxes $F < 10^{-17} cm^{-2} s^{-1} sr^{-1}$ for $10^{-4} < \beta < 10^{-3}$. The scenario for the interpretation of the mica results is sketched in Fig. 20.

Although the mica experiments offer a clever way of challenging astrophysical limits, they are indirect methods and there are several reasons why they might not be sensitive to monopoles. For example, if monopoles have a positive electric charge (dyon) or have protons attached, as suggested by Bracci and Fiorentini [74], then Coulomb repulsion would prevent capture of heavy nuclei and tracks would not be formed in mica. A long range force due to extra angular momentum carried by a monopole-electric charge system could reduce the probability for a monopole to capture a nucleus. Also, if monopoles catalyze nucleon decay with a large cross section, monopole-nucleus bound states could be short lived.

7.4. Searches in bulk matter

These types of searches represent a continuation of those reported in Section 5.2, but on a much larger scale.

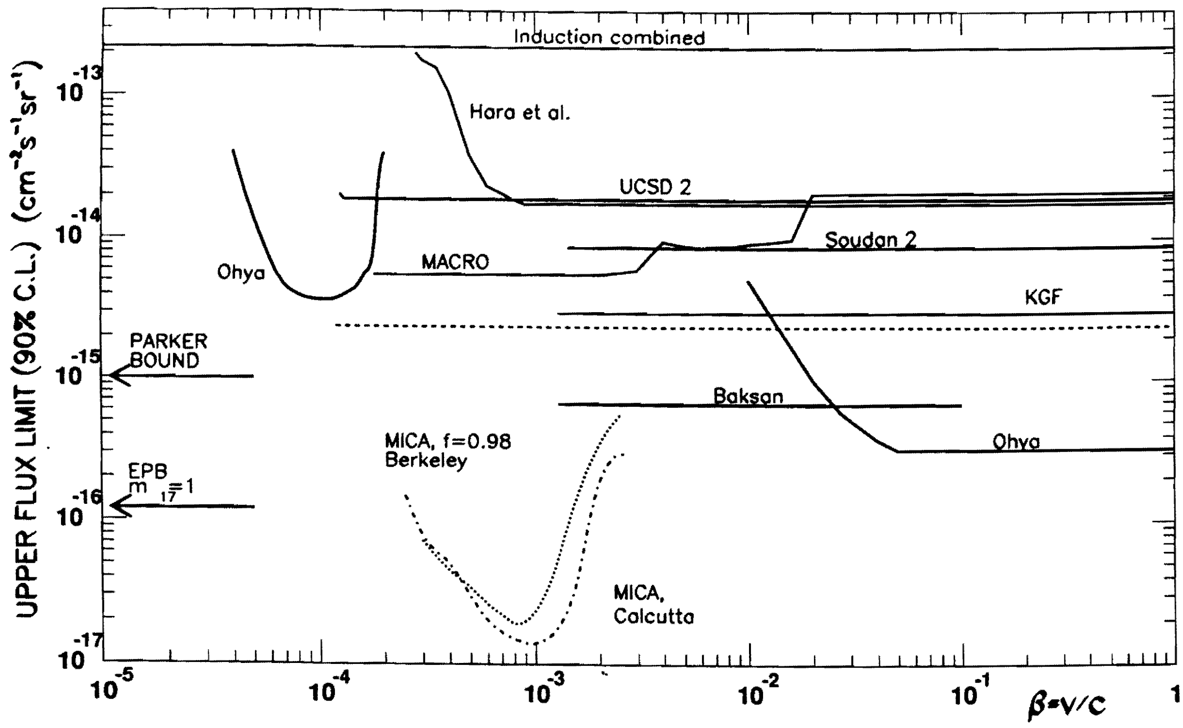

Figure 19 - Compilation of 90% C.L. experimental upper limits on a monopole flux reaching the Earth [65–66,71–73]. Solid lines indicate direct searches, dotted and dashed lines MICA experiments; for the dashed line see text of Section 10.

A Kobe group performed a search for relic monopoles trapped in iron sand using several tens of kilograms of material formed between 10^7 and 10^8 years ago [75]. The sand was heated above the Curie point, at which temperature the material stops being ferromagnetic. The poles trapped in the material would leave it, would fall towards the Earth and would be detected in a superconducting induction coil through which they would pass. The Kobe group placed the upper limit of $2 \cdot 10^{-6}$ poles per gram of ore. It is difficult to extract from this an upper limit on the monopole flux: it was estimated to be of the order of 10^{-13} poles $cm^{-2}s^{-1}sr^{-1}$ for poles with $\beta < 10^{-4}$. The sensitivity is much better for "classical" monopoles or for poles with an intermediate mass.

8. Monopole catalysis of proton decay

A GUT monopole may catalyze proton decay, $p + M \to M + e^- + \pi^0$. It was originally thought that the cross-section for this process would be very small, of the order of the size of the monopole core ($\simeq 10^{-58} cm^2$), where may be found the virtual particles which mediate the $\Delta B \neq 0$ interactions. In 1982 Rubakov and

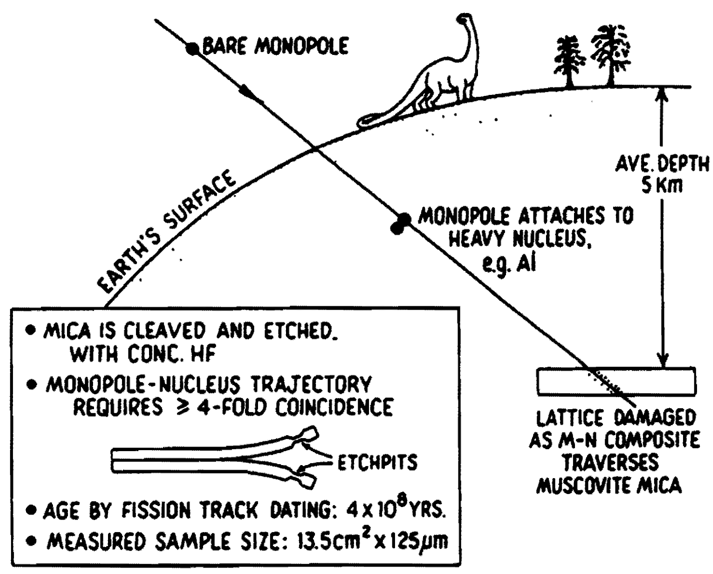

Figure 20 - Scenario hypothesized for the interpretation of the mica experiments [72,73].

Callan [76,77] showed that the cross-section is independent of the monopole mass and could be comparable with the cross-section of ordinary strong interactions, because the monopole core should be surrounded by a fermion-antifermion condensate (Fig. 2), with some $\Delta B \neq 0$ terms extending up to the confinement region.

The catalysis cross section for protons is roughly given by [4]

$$\sigma_{cat} \simeq \sigma_R \; 0.62/\beta \quad mbarn \tag{20}$$

where σ_R quantifies our ignorance.

The cross section for the capture of a nucleus by a monopole is

$$\sigma_{capt} \simeq 10^{-3}/\sqrt{\beta} \quad mbarn \tag{21}$$

Notice that $\sigma_{cat} \geq \sigma_{capt}$ for $\beta \leq 4 \cdot 10^{-3}$. Thus the monopole captures a proton or a nucleus and subsequently one should have the catalysis reaction. In most experiments there are no free protons, but heavier nuclei, like Oxygen (in H_2O) or Fe. Arafune [78] and Craigie [4] have shown that for spin 1/2 nuclei, like aluminium, there should be an enhancement in the cross section over that for free protons. Instead for spin-0 nuclei there should be a strong β-dependent suppression. For oxygen the suppression factor could be of the order of 10^{-2} at $\beta = 10^{-3}$, $\simeq 10^{-5}$ at $\beta = 10^{-4}$; the factor should be somewhat larger for iron ($\simeq 2 \cdot 10^{-6}$ for $\beta = 10^{-4}$).

If the $\Delta B \neq 0$ cross-section for monopole catalysis of proton decay were large, then a monopole would trigger a chain of baryon "decays" along its passage through a large detector, such as those designed to study baryon decay. The mean free path

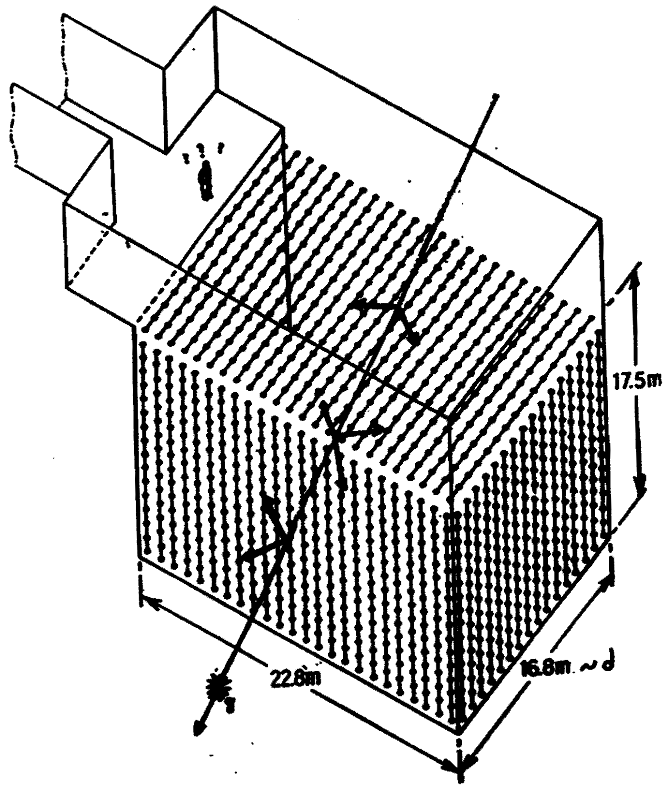

Figure 21 - Experimental signature of a string of monopole induced proton decays in the IMB water Cherenkov detector [79]. The early electronics of the large proton decay detectors was insensitive to proton decay candidates happening a short time after the first candidate.

$\lambda = (N_o \rho \sigma)^{-1}$ between two successive monopole-induced proton decays would be, for slow monopoles,

$$\lambda_c = \frac{1}{N_o \rho \sigma_{cat}} \simeq \frac{4200}{\sigma(gcm^{-3})} \cdot \frac{\beta}{\sigma_R} \tag{22}$$

where N_o is Avogadro's number and ρ is the density of the material in g cm^{-3}. For $\beta = 10^{-3}$, assuming $\delta_R \sim O(1)$, the mean free path would be 4.2, 420, 42000 cm for $\sigma_R = 1$, 10^{-2} and 10^{-4}, respectively. The time between two successive monopole-induced proton decays would be

$$\tau = \frac{\lambda}{\beta c} = \frac{1}{c N_A \rho \sigma_{cat} \sigma_R} \simeq \frac{1.4 \cdot 10^{-7}}{\sigma_R \rho (gcm^{-3})}. \tag{23}$$

For $\beta = 10^{-3}$ one has $\tau = 1.4 \cdot 10^{-7}$, $1.4 \cdot 10^{-5}$ and $1.4 \cdot 10^{-3}$ s for $\sigma_R = 1$, 10^{-2} and 10^{-4}, respectively.

As soon as the idea of monopole catalysis of proton decay became known, some rough upper limits were established from bubble chamber information and some quick experiments were performed. Astrophysical limits were established. Later, all large-scale proton decay experiments added new triggers to be sensitive to multiple

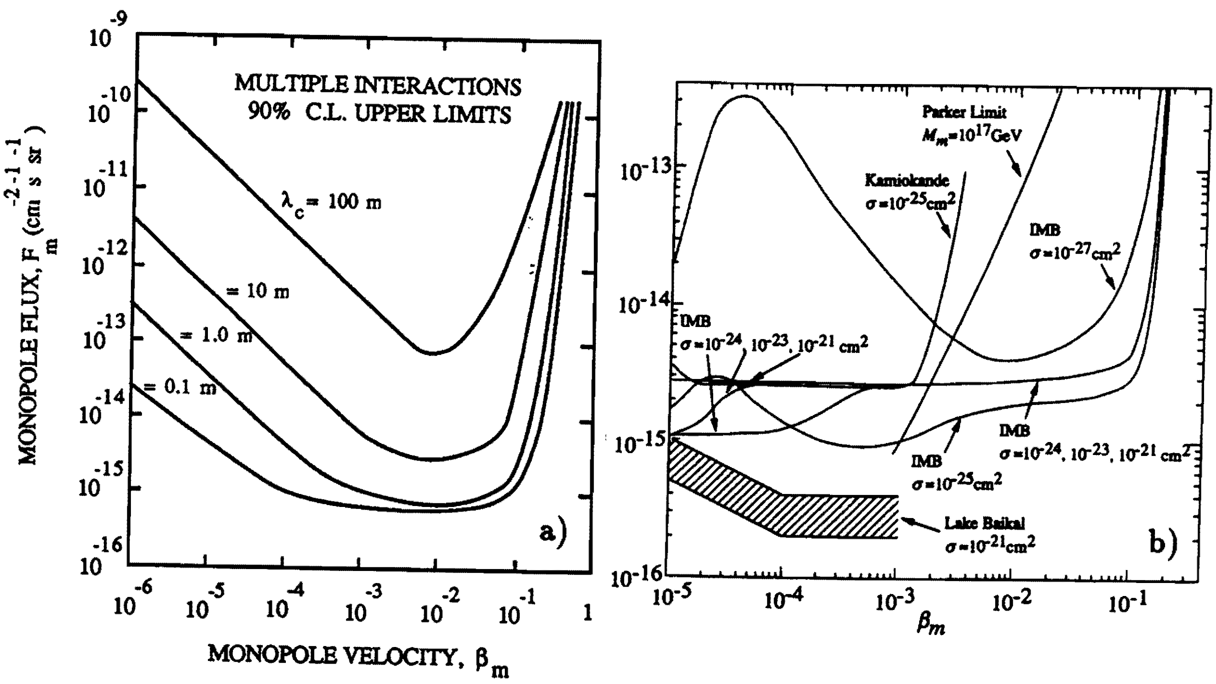

Figure 22 - (a) Upper limits (90% c.l.) on the monopole flux vs. monopole velocity for the multiple catalysis of proton decay in the IMB water Cherenkov detector for several values of the catalysis cross-section [79]. (b) Limits from "multihit" analyses from different detectors [79].

"proton decays". The signature for a monopole-catalyzed nucleon decay should be different from that of a spontaneous nucleon decay. In the last case the laboratory momentum has to be balanced, which leads to tracks in a back-to-back configuration. In the case of monopole-induced decays, the events may have the same general appearance of low-energy ($\simeq 1-2$ GeV) atmospheric neutrino interactions in the detector.

No string of events consistent with monopole catalysis of nucleon decay was found. Upper limits were established by the KGF, Mt. Blanc, Kamioka, IMB, Soudan 1 and Frejus experiments, some of which will now be shortly reviewed.

The Irvine-Michigan-Brookhaven (IMB) water Cherenkov detector [79] was a parallelepiped of $(17 \times 22.5 \times 18) m^3$, viewed by 2048 photomultipliers, Fig. 21. It was located at a depth of 2000 m.w.e. in the Morton salt mine near Cleveland, Ohio. The upper limits obtained for the catalysis of proton decay are shown in Fig. 22. The best upper limit is $F \leq 10^{-15} cm^{-2}s^{-1}sr^{-1}$ for $\sigma_{cat} = 100\ mbarn$ for β around 10^{-3} [79], see Fig. 22.

The Kamiokande water Cherenkov counter is a cylinder of 15 m diameter and 16 m height (3000 t of water, about 1000 t fiducial mass) viewed by 1000, 20" photomultiplier tubes (specifically designed for the experiment) which cover 20% of the outer surface of the detector. The apparatus is placed in the Kamioka mine at a depth of 2700 m.w.e.. They obtained an upper limit $F < 7 \cdot 10^{-15} cm^{-2}s^{-1}sr^{-1}$ (for $\sigma_c = 10\ mbarn$ and $(1/\beta^2)$-dependence) (Fig. 23) [80]. A much larger water detector (Superkamiokande) is under construction in the same mine [80], see Fig. 23.

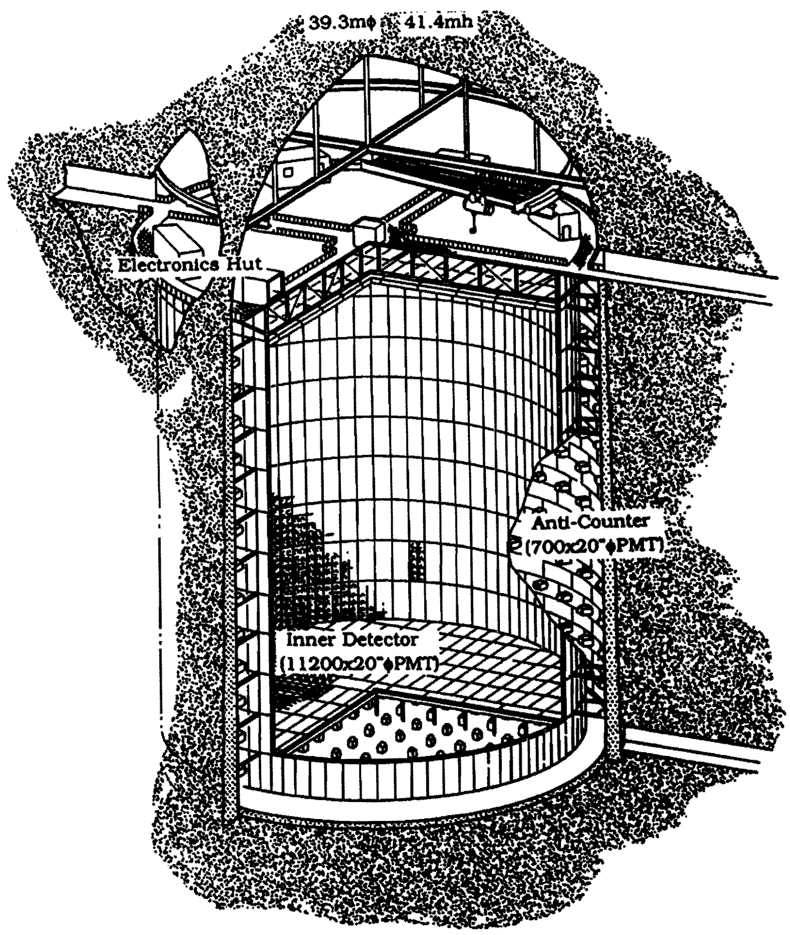

Figure 23 - Layout of the Superkamiokande detector [80] (under construction).

A deep underwater detector, located at Lake Baikal [81], consists of 6 photomultiplier modules and one electronics module deployed at a depth of $\sim$ 1 km. The detector is sensitive to catalysis of proton decay in the $10^{-5} < \beta < 10^{-4}$ range for $\sigma_{cat} > 1000$ *barn*; it yielded $F < 7 \cdot 10^{-15} cm^{-2} s^{-1} sr^{-1}$. The low trigger efficiency of the detector limits its β-range and its sensitivity to large catalyses cross sections. Dumand [82] and Nestor [83] are similar detectors which are being deployed, the first in the Pacific, close to the Haway islands, the second close to the coast of Greece, in the Mediterranean sea. Amanda is a detector which is being tested in the deep ice of Antarctica [84].

It should be noted that if the Rubakov-Callan effect exists, the monopole-proton composites are unstable.

8.1. Astrophysical limits from monopole catalysis of nucleon decay

The number of monopoles inside a star or a planet should keep increasing with time, because of a constant capture rate and of a probably small pole-antipole annihilation rate. The catalysis of nucleon decay by magnetic monopoles could be another source of energy for these astrophysical bodies.

The catalysis argument, applied to the protons of our Sun, leads to the possibility that the Sun could emit electron neutrinos, with an average energy of 35 MeV, coming from muon decays. This process could lead to about $3 \cdot 10^4$ electron neutrinos incident on the Earth per cm^2 per second if $\simeq 1\%$ of the solar luminosity is due to monopole catalysis. The electron neutrinos could be detected in a terrestrial apparatus through their elastic scattering on electrons. The Kamioka proton decay detector is sensitive to electrons with energies larger than about 8 MeV. From three possible candidates the authors estimate an upper limit $F < 8 \cdot 10^{-10} \beta^2$ if the monopole catalysis cross-section is 1 *mbarn* (the expected background from atmospheric neutrinos with $E_\nu \simeq 35$ MeV is about 1 event). From limits of this sort one could place a limit on the number of poles in the Sun, at the level of less than 1 pole per $10^{12} g$ of solar material [8].

A speculative upper bound on the total number of monopoles present inside the Earth may be made assuming that the energy released by monopole catalysis of nucleon decay in the Earth should not exceed the surface heat flow [8]. The Earth should stop monopoles with $\beta < 10^{-4}$; the stopped monopoles will go towards the centre of the Earth, where they could have drift velocities of the order of $\beta_d \simeq 10^{-5}$. At these low velocities the catalysis cross-section may have reached a constant value, $\sigma_c \simeq 10^{-28} \sigma_R$. One obtains a limit for the product $\beta_d \sigma_R F$:

$$\beta_d \sigma_R F < 10^{-20} cm^{-2} s^{-1} sr^{-1}. \tag{20}$$

If $\sigma_R = O(1)$, this could be a strong bound; but in iron there could be a suppression factor of $\simeq 2 \cdot 10^{-6}$ for $\beta = 10^{-4}$.

9. Other types of searches

Most of the experiments and of the discussions made in the previous sections concern magnetic monopoles with one or more units of Dirac charge and with masses of the order of 10^{17} GeV (GUT poles) or smaller than 850 GeV (classical Dirac poles). Superconducting induction detectors are sensitive to poles of any speed, while other detectors are generally sensitive to poles with $\beta \geq 10^{-4}$.

Magnetic monopoles with an electric charge (dyons) may also exist [85]. They may arise as quantum mechanical excitations of magnetic monopoles (In addition, one should consider monopole-proton and monopole-nucleus bound states). In general the dyon mass is expected to be larger than that of poles with no electric charge. Thus dyons may have already decayed into ordinary poles. Direct searches for dyons in the penetrating cosmic radiation may be performed as for normal poles, bearing in mind that the Drell effect may be much less effective in the case of positive dyons.

Among other searches one may mention the searches for protons with a monopole-antimonopole structure, the searches for magnetic currents and the searches for tachyon monopoles, that is for monopoles which should be travelling faster than light.

In a number of early papers, Ehrenhaft described some experiments in which he said to have observed magnetic charges [86]. In these experiments, aerosols of ferromagnetic microparticles (iron, nickel, cobalt) when weighted in a gas atmosphere and subjected at the same time to a uniform magnetic field and to a beam of light, move like objects carrying magnetic charges. These observations need explanations.

Among other methods proposed for monopole searches we may recall that based on searches for anomalies in the maser emission of large interstellar clouds of OH molecules. The monopoles may change the scale of splitting of Zeeman sublevels or change the polarization of one optical line (from circular to linear). The effects depend on the square of the magnetic charge [87].

A number of authors have conjectured that monopoles could be tachyons, that is faster-than-light particles. For instance Parker proposed an extended Lorentz transformation relating momenta and fields in the rest field of the tachyon to quantities observable in the laboratory frame [88,89]. The transverse fields of an electrically charged tachyon with charge q=e moving with infinite speed appear in the laboratory frame as a magnetic field like that produced by a particle with a magnetic charge g=e. Thus in this case the charge of the monopole is expected to be much smaller than the Dirac one. Superluminal and subluminal particles may interact electromagnetically with photons and thus with each other. As a consequence the cross section for the backward scattering of photons by photons should be twice as large as is predicted without taking into account tachyon monopoles.

Experimental searches for tachyon monopoles [47] were based on several hypotheses: a) production by $\simeq 1$ MeV γ-rays in ordinary matter; b) no absorption in several centimeters of material (Pb); c) acceleration in a magnetic field; d) emission of electromagnetic Cherenkov radiation in vacuum and e) magnetic charge equal to the Dirac value. According to Mignani et al. at least one of these hypotheses is inconsistent with the others and thus the meaning of the limits obtained by these searches is not clear [88].

Most experiments cannot establish if the magnetic-dipole moment of the proton is made from a monopole-antimonopole distribution rather than from a distribution of current loops or of intrinsic moments, since the experiments are sensitive only to the proton's magnetic field outside the distribution [90,91]. An exception is the hyperfine transition in the neutral hydrogen atom which leads to the emission of the 21 cm wave. The interaction energy between the electron and proton magnetic moments is of the form $W = -A\vec{\mu_e} \cdot \vec{\mu_p}$ where $A = (-4\pi/3)(\psi(0))^2$ for the normal proton ($\psi(0)$ is the wave function at the origin); it would be twice as large for a proton dipole moment equal to the observed one, but arising from a monopole-antimonopole distribution. In this case the hyperfine transition would lead to a 42 cm radiation. The fact that ordinary matter leads to the 21 cm radiation and not to the 42 cm one is a result which seems to deny magnetic charge any role in the structure of ordinary matter. If one assumes that the magnetic moment of the proton is given by a normal part term and by a second term $\mu' = \delta\mu_p$ due to a pole-antipole structure, then the precision measurement of the 21 cm wave yields the limit $\delta < 2 \cdot 10^{-6}$. If one writes $\mu' = g_D d = \delta\mu_p$, one obtains $d < \delta\mu_p/g_D = 10^{-8} fm$. There remains the logical possibility that some small fraction of protons could be anomalous and have their moments made from magnetic-charge distributions rather than from current distributions. In this case there is no real guarantee that the magnetic-dipole moment would be numerically equal to the normal one, but one has to hypothesize the equality. Broderick et al. analysed the radiation emitted by three strong sources of continuum emission, with a strong absorption line at the 21 cm radiation [91]. The absorption is interpreted as due to neutral galactic hydrogen located in the line of sight from the sources to the detecting radiotelescope. The authors did not find any absorption at 42 cm. Thus they excluded the presence of anomalous protons in the neutral galactic hydrogen at a level of $2 \cdot 10^{-4}$ of the normal protons.

10. Outlook and conclusions

Simple searches for "classical" monopoles will probably continue to be performed also at the new higher energy accelerators. But most searches will concentrate on supermassive monopoles in the cosmic radiation. While the early searches for a flux of GUT monopoles involved small and simple equipments, the present direct searches involve a small number of large detectors, see Table 6.

Superconducting induction detectors. There was a trial to make a co-operative effort for a detector with $S\Omega \simeq 1000\ m^2 sr$, but it did not proceed further.

Track-etch detectors. In the Kamioka mine a Japanese group used about 2000 m^2 of CR39 nuclear track detector [24]. A similar system of more than 1200 m^2 has being installed in the MACRO experiment at Gran Sasso [71].

Electronic experiments. The Baksan scintillator detector has $S\Omega = 1800\ m^2 sr$; Soudan 2 proton decay experiment has $S\Omega \simeq 3000\ m^2 sr$ [67] (see Subection 7.2 and Figs. 15,16).

The LVD experiment at Gran Sasso using scintillators and limited streamer tubes [70] will have $S\Omega \sim 5000\ m^2 sr$, see Fig. 17 and Table 6. Each of the 41 scintillator modules shown in Fig. 17 is made of 8 scintillation counters, each of $1 \times 1 \times 1.5\ m^3$ and viewed by 3 photomultipliers.

The MACRO experiment at Gran Sasso has as a specific search for monopoles one of his main aims [71]. The main part of the MACRO detector is a horizontal structure consisting of a lower part with two layers of liquid scintillation counters, ten layers of limited streamer tubes and a layer of CR39 track-etch detectors (see Fig. 18 and Table 6). The upper part (the "attico") has a third layer of liquid scintillators and 4 layers of limited streamer tubes. The four vertical sides are closed by one layer of liquid scintillation counters and six layers of limited streamer tubes. The active dimensions of the detector are $12\ m \times 9.5\ m \times 76\ m$. The acceptance of this closed structure for an isotropic particle flux is about 10.000 $m^2 sr$. The acceptance is sufficiently large to push a direct search to about $10^{-16} cm^{-2} s^{-1} sr^{-1}$. The experiment has enough redundancy of information to attain reliable interpretations on the basis of a few events. With the use of complementary techniques the experiment gains in "convincingness" and explores different monopole detection mechanisms. The range of β covered is $\beta \geq 10^{-4}$ in different types of detectors. Monopoles are searched for by requiring correlated and long light pulses on 3 different scintillation counters, which have an energy loss threshold of 0.1 minimum ionizing. The streamer tube system searches for magnetic monopoles by using both the standard ionization mechanism as well as the Drell-Penning effects in $He - C_5H_{10}$. A monopole candidate is signalled by a spatial track through several tube layers with hits appearing in a slow time sequence. The system provides three dimensional tracking of penetrating particles with a spatial accuracy of 1 cm and the resolution of two tracks with separation $\simeq 5cm$. A multiple trigger system ensures that the whole range for $\beta > 10^{-4}$ is covered in a redundant way. The electronics and the data acquisition system is distributed along the apparatus. Three layers of CR39 nuclear track detectors are inserted horizontally in the middle of the lower detector and on the north and east vertical walls. The array is modular so that local sections can be removed and scanned for candidate tracks. Due to their sensitivity to different components of the energy loss process, the CR39 detectors will provide sensivity in $4 \times 10^{-5} < \beta < 3 \times 10^{-4}$ and for $\beta > 3 \times 10^{-3}$. The published limits have been obtained with part of the apparatus, when it was under construction (the data taken should allow to reach the limit sketched by the dashed line in Fig. 19).

Catalysis of proton decay. Proton decay experiments are able to detect a string of catalyzed nucleon decays. The present Kamiokande and the future Superkamiokande water Cherenkov detectors have this capability.

In conclusion: we still have good theoretical reasons to believe that magnetic monopoles may exixt in nature, though no good candidate has been found. The size and quality of the experiments are now capable of reaching with certitude about an order of magnitude below the Parker limit.

Table 6 - Overall Comparison of large Monopole Search Experiments (direct searches). For the scintillation detectors the table gives the total number of counters. l.s.t. = limited streamer tubes.

Experiment	Detection Method				$S \cdot \Omega$ ($m^2 sr$)
	Induction	*Scintill. counters*	*Gas*	*Track Etch*	
Baksan	–	3200	–	–	~ 1800
Kamioka	–	–	–	CR-39	~ 6000
MACRO	–	572	$He + C_5H_{10}$ l.s.t.	CR-39	~ 10000
Soudan 2	–	–	fine grained cal.	–	~ 3000
LVD	–	650-1600	limited str. tub.	–	≤ 5000

Acknowledgements.

I would like to acknowledge many colleagues for cooperation, explanations and discussions. In particular I thank B. Barish, P. Capiluppi, R.A. Carrigan Jr., S. Cecchini, H. Dekhissi, G. Fiorentini, M. Grassi, G. Mandrioli, L. Patrizii, V. Popa, G. Pugliese, A.M. Rossi, A. Sciubba, P. Serra, P. F. Spada, M. Spurio, J. Stone and G. Tarlé. I wish to thank Mrs. B. Simoni-Bonacorsi for typing the manuscript.

11. References

(For more extensive early references the reader is referred to [4,5,8,49]).

1. P.A.M. Dirac, Proc. R. Soc. London 133 (1931) 60; Phys. Rev. 74 (1948) 817.
2. G. 'T Hooft, Nucl. Phys. B79 (1974) 276.
3. A. M. Polyakov, JETP Lett. 20 (1974) 194.
4. N. Craigie, G. Giacomelli, W. Nahm and Q. Shafi, Theory and Detection of Magnetic Monopoles in Gauge Theories, World Scientific (1986).
5. G. Giacomelli, Riv. Nuovo Cimento 7 (1984) 1.
6. B. Cabrera, Phys. Rev. Lett. 48 (1982) 1378.
7. G. Giacomelli (Conference high-lights and summation. Experimental) "Monopoles 83" Workshop, Ann Arbor, Mich. (1983).
8. G. Giacomelli, Status of Monopole Searches, Invited paper at the 9^{th} Workshop on Gran Unification, Aix-les-Bains (1988);
   Review of Particle Properties - Magnetic Monopole Searches, Phys. Rev. D45 (1992) N. 11.
9. L. Bracci et al., Phys. Lett. B124 (1983) 29, 493; B258 (1985) 726.
10. G. F. Drell et al., Nucl. Phys. B209 (1982) 45.
11. S. P. Ahlen, Rev. Mod. Phys. 52 (1980) 121;
    C. Goebel (Binding of monopoles to nuclei). Proceeding of the Monopole Workshop, Ann Arbor, Mi, (1983);
    D. M. Ritson, SLAC-Pub-2950 (1982) (unpublished).
12. S. P. Ahlen and K. Kinoshita, Phys. Rev. D26 (1982) 2347.
13. S. P. Ahlen and G. Tarlè, Phys. Rev. D27 (1983) 688.
14. L. Bracci, G. Fiorentini and R. Tripiccione, Nucl. Phys. B238 (1984) 167.
15. B. Cabrera and W.P. Trower, Found. Phys. 13 (1983) 195.
16. J. L. Stone, Magnetic Monopoles Search Experiments, UM HE 85-02 (1985);
    J. L. Stone, Magnetic Monopoles Search, 2^{nd} School on Non-Accelerator Particle Astrophysics, Trieste (1991).
17. J. D. Ficenec et al., Phys. Rev. D36 (1987) 311.
18. G. Battistoni et al., Nucl. Instr. Meth. 163 (1979) 93.
19. MACRO Collab., S. Ahlen et al., Nucl. Instr. Meth. A324 (1993) 337.
20. P. B. Price et al., Phys. Rev. Lett. 35 (1975) 487; Phys. Rev. D18 (1978) 1382; Phys. Rev. Lett. 52 (1984) 1265.
21. S. P. Ahlen et al., (Track recording solids) Phys. Today, Sept. 1981, 32.
22. K. Kinoshita, P.B. Price and D. Fryberger, Phys. Rev. Lett. 48 (1982) 77.
23. P. B. Price, Phys. Lett. B140 (1984) 112.
24. T. Doke et al., Nucl. Instr. Meth. B34 (1988) 81;
    S. Orito, Phys. Rev. Lett. 66 (1991) 1951; and private communication.
25. D. P. Snowden - Ifft and P.B. Price, Phys. Lett. B288 (1992) 250.
26. S. Cecchini et al., 16^{th} Int. Conf. Particles Tracks in Solids, Beijng (1993), DFUB 93-3; "Calibration with relativistic and low velocity ions of the CR39 nuclear track detector used in MACRO", Nucl. Instr. Meth., to be published (1994).
27. M. Fidecaro, G. Finocchiaro and G. Giacomelli, Nuovo Cimento 22 (1961) 657.

28. E. Amaldi et al., Nuovo Cimento 28 (1963) 773.
29. K. Kinoshita et al., Phys. Rev. D46 (1992) R881.
30. P. Musset, M. Price and E. Lohrmann, Phys. Lett. B128 (1983) 333.
31. J. L. Pinfold et al., Phys. Lett. B316 (1993) 407.
32. G. Giacomelli et al., Nuovo Cimento A28 (1975) 21.
33. H. Hoffmann et al., Lett. Nuovo Cimento 23 (1978) 357.
34. B. Aubert et al., Phys. Lett B120 (1983) 465.
35. P. B. Price et al., Phys. Rev. Lett. 65 (1990) 143.
36. M. Bertani et al., Europhysics Lett. 12 (1990) 613.
37. I. I. Gurevich et al., Phys. Lett. 31 (1970) 394.
38. R. A. Carrigan jr., B.P. Strauss, G. Giacomelli, Phys. Rev. D17 (1978) 1754.
39. J. M. Barkov et al., Search for Dirac monopoles in pN collisions at 400 GeV/c, CERN/EP 83-194 (1983).
40. M. Schein, D.M. Haskin and R.G. Glasser, Phys. Rev. 99 (1955) 643.
41. G. B. Collins et al., Phys. Rev. D8 (1973) 892.
42. D. L. Burke et al., Phys. Lett. B60 (1975) 113.
43. L3 Collab., S.S. Ting, Presentation at the LEPC, February 1994.
44. L. Karlsson, Nucl. Instr. Meth. 116 (1974) 275.
45. R. L. Fleischer et al., Phys. Rev. 177 (1969) 2029.
46. R. A. Carrigan jr., F. A. Nezrick, B. P. Strauss, Phys. Rev. D13 (1976) 1823.
47. D. F. Bartlett et al., Phys. Rev. 180 (1978) 2253; D24 (1981) 612.
48. G. Giacomelli, Experimental status of monopoles, in Proc. of the Workshop on Magnetic Monopoles, Wingspread (1982).
49. G. Giacomelli, Magnetic Monopoles, 3^{rd} School on Non-Accelerator Particle Astrophysics, Trieste (1993).
50. J. Ruzicka and V.P. Zrelov, Dubna Preprint D2-81-675 (1981).
51. E. N. Parker, Ap. J. 160 (1970) 383.
52. M. S. Turner et al., Phys. Rev. D26 (1982) 1296.
53. F. C. Adams et al., Phys. Rev. Lett. 70 (1993) 2511.
54. Y. Raphaeli and M.S. Turner, Phys. Lett. B121 (1983) 115.
55. Th. W. Rujgrok et al., (Monopole Chemistry), DESY 83-036 (1983).
56. S. W. Barwick, K. Kinoshita and P. B. Price, Phys. Rev. D28 (1983) 2838.
57. B. Cabrera et al., Phys. Rev. Lett. 64 (1990) 835;
R. D. Gadner et al., Phys. Rev. D44 (1991) 622;
M. E. Huber et al., Search for a flux of cosmic ray magnetic monopoles with an 8-channel superconducting detector, Phys. Rev. D44 (1992) 636.
58. J. Incandela et al., Phys. Rev. Lett. 53 (1984) 2067; Phys. Rev. D34 (1986) 2637.
59. C. C. Chi, Monopole search at IBM: present status and future plans, Invited paper at the Monopole '83 Workshop, Ann Arbor, Mich. (1983);
S. Bermon et al., Phys. Rev. Lett. 55 (1984) 1850; 64 (1990) 839.
60. C. D. Tesche et al., Appl. Phys. Lett. 43 (1983) 839.
61. P. Musset, Monopole searches, Physics Underground Workshop, St. Vincent, Italy (1985), Nuovo Cimento C9 (1986) 559.
62. J. C. Schonten et al., J. Phys. E220 (1987) 850;
A. D. Caplin et al., Nature 317 (1985) 234; 321 (1986) 402.

63. M. W. Cromar et al., Phys. Rev. Lett. 56 (1986) 2561.
64. R. Bonarelli et al., Phys. Lett. B112 (1982) 100; B126 (1983) 137;
T. Moshimo et al., J. Phys. Soc. Jpn. 51 (1982) 3065; Phys. Lett. B128 (1983) 327;
D. E. Groom et al., Phys. Rev. Lett. 50 (1983) 573;
B. Barish et al., Phys. Rev. D36 (1987) 2641.
65. E. N. Alexeyev et al., Lett. Nuovo Cimento 35 (1982) 413; Proceedings of the 1990 Int. Cosmic Ray Conf., Adelaide (1990).
66. J. D. Ullmann et al., Phys. Rev. Lett. 47 (1981) 289;
Mt. Blanc 1 Collab., G. Battistoni et al., Phys. Lett. B133 (1983) 454;
F. Kajino et al., Nucl. Phys. 10 (1984) 447; Phys. Rev. Lett. 52 (1984) 1373;
Soudan 1Collab. J. Bartelt et al., Phys. Rev. D36 (1987) 1990;
S. Diego Collab., G. Masek et al., Phys. Rev. D35 (1987) 2758;
Akeno Collab., T. Hara et al., Phys. Rev. Lett. 56 (1986) 553; 21^{st} Int. Conf. Cosmic Rays, Adelaide (1990);
M. E. Huber et al., Phys. Rev. Lett. 64 (1990) 835.
67. J. L. Thron et al., Phys. Rev. D46 (1992) 4846.
68. Frejus Collab., Ch. Berger et al., Nucl. Phys. B313 (1989) 509; Z. Phys. C50 (1991) 385; Phys. Lett. B240 (1990) 237; B269 (1991) 227.
Y. Benadjal (Search for magnetic monopoles with the Frejus detector) LAL-89-69, Doctoral Thesis.
69. KGF Collab., Krishnaswamy et al., Phys. Lett. 142B (1984) 99; Nuovo Cimento 9C (1986) 167.
70. LVD Collab., C. Castagnoli et al., Nuovo Cimento (1985);
Kitami Collab., T. Doke et al., Phys. Lett. B129 (1983) 370; Nucl. Tracks. Rad. Meas. 8 (1984) 609;
S. Tasaka and T. Suda, J. Phys. Soc. Jpn. 55 (1986) 3749.
71. MACRO Collab., S. Ahlen et al., Phys. Rev. Lett. 72 (1994) 608;
J. Hong (Search for GUT magnetic monopoles and other supermassive particles with the MACRO detector) Caltech PhD Thesis (1993);
M. Spurio (Ricerca di monopoli magnetici nell'esperimento MACRO al Gran Sasso) Tesi di Dottorato, University of Bologna (1990).
72. P.B. Price et al., Phys. Rev. Lett. 59 (1987) 2523.
73. D. Ghosh and S. Chatterjea, Europhys. Lett. 12 (1990) 25.
74. L. Bracci and G. Fiorentini, Phys. Lett. B124 (1983) 493.
75. T. Ebisu and T. Watanabe, J. Phys. Soc. Jpn. 52 (1983) 2617.
76. G. G, Callan, Phys. Rev. D26 (1982) 2058.
77. V. A. Rubakov, JETP Lett. 33 (1981) 644; Nucl. Phys. B203 (1982) 311.
78. J. Arafune and M. Fukugita, Phys. Rev. Lett. 50 (1983) 1901.
79. R. Becker-Szendy et al., Phys. Rev. D49 (1994) 2169.
80. Kamiokande Collab., K. S. Hirata et al., Phys. Lett. B220 (1989) 308; B311 (1993) 357;
Superkamiokande Collab., Y. Suzuki et al., Proceed. of 11^{th} Moriond Workshop and ICRR Report 247-91-16 (1991).

81. Baikal Collab., L. B. Bezroukov et al., Proceedings of Int. Conf. on High En. Phys., Leipsig (1984); S. D. Alatin, Proceedings of Int. Conf. on Trends in Astroparticle Phys., Aachen (1991).
82. Dumand Collab., C. M. Alexander et al., Proceedings of the Int. Symp. on UHE Cosmic Ray Interact., Ann Arbor, Mi, UWSEA PUB 92-15 (1992).
83. Nestor Collab., E. Anassoutris et al. (A neutrino Particle Astrophysics Underwater detector lab. for the Mediterranean) Proceed. of H.E. Neutrino Astroph. Workshop, Hawaii (1992).
84. Amanda Collab., P. B. Price, Seminar (1993).
85. J. Preskill, Ann. Rev. Nucl. Part. Sci. 34 (1984) 461.
86. F. Ehrenhaft, Phys. Zs. 31 (1930) 478; Phys. Rev. 65 (1944) 62.
87. S. G. Rautian et al., Phys. Lett. B70 (1977) 278.
88. E. N. Parker, Astrophys. J. 160 (1970) 383.
89. R. Mignani and E. Recami, Lett. Nuovo Cimento 13 (1975) 589.
90. M. Bonnardeau and A.K. Drukier, Astrophys. Space Sci. 60 (1979) 375.
91. J. J. Broderick et al., Phys. Rev. D19 (1979) 1046.